Design Study of Flapping Foil Propulsion for an Odyssey Class Autonomous Underwater Vehicle

by

Rafael A. Mandujano

Submitted to the Department of
Mechanical Engineering in Partial
Fulfillment of the Requirements for the
Degree of

Bachelor of Science

at the

Massachusetts Institute of Technology

June 2002

© 2002 Rafael Mandujano
All rights reserved

MASSACHUSETTS INSTITUTE OF TECHNOLOGY
JUN 17 2003
LIBRARIES

The author hereby grants to MIT permission to reproduce and to distribute publicly paper and electronic copies of this thesis document in whole or in part.

Signature of Author.....
Department of Mechanical Engineering
May 10, 2002

Certified by.....
Chryssostomos Chryssostomidis
Professor of Ocean Engineering
Thesis Supervisor

Certified by.....
Justin Manley
Research Engineer
Thesis Supervisor

Accepted by.....
Ernest Cravalho
Chairman, Undergraduate Thesis Committee

ARCHIVES

Design Study of Flapping Foil Propulsion for an Odyssey Class Autonomous Underwater Vehicle

by

Rafael A. Mandujano

Submitted to the Department of Mechanical Engineering
on May 10, 2002 in Partial Fulfillment of the
Requirements for the Degree of Bachelor of Science in
Mechanical Engineering

ABSTRACT

A design study was conducted to examine the feasibility of implementing fish-like flapping foil propulsion on an Odyssey Class autonomous underwater vehicle (AUV). Theoretically, fish-like propulsion offers higher efficiencies, greater maneuverability, and the potential for faster accelerations than the conventional propulsion system currently in use on the Odyssey Class AUV. Previous laboratory research has shown promising results, and retrofitting an Odyssey Class AUV with a flapping foil is a cost-effective way to step up the learning curve toward applying this technology in a field setting.

Based primarily on MIT's RoboTuna research on the swimming motions of fish, the proposed design hopes to achieve a speed of 1.5 m/s. Oscillating two tail links independently at a tail flapping frequency of about 1 Hz should provide this performance. The links are driven with DC brushless motor systems through a Scotch yoke linkage and a linear actuator. Pitch and roll motion is accomplished with the addition of servo actuated pectoral fins, while dorsal and anal fins provide additional directional stability. A variety of motion schemes were contemplated, but the final design was chosen with an emphasis on simplicity, practicality, and robustness for use in a field setting.

Thesis Supervisor: Chryssostomos Chryssostomidis
Title: Professor of Ocean Engineering

Thesis Supervisor: Justin Manley
Title: Research Engineer

Acknowledgements

I gratefully acknowledge the weekly support of Justin Manley for his patience and guidance throughout the entire process of conceiving, developing, and writing this thesis. Thanks also go out to Professor Chryssostomidis for his supervision, Sam Desset for taking time to answer my many questions, and everyone at Sea Grant for their supportive attitude.

I would also like to think back to the beginning and thank Tom Consi for pointing me in the direction of several labs, and ReRe Quinn, without whom I never would have gotten all my paperwork in on time.

Contents

List of Figures

Section 1

An Introduction to AUVs and Propulsion

1.1 The AUV Mission

Autonomous underwater vehicles (AUVs) are submersible vehicles that contain their own power and operate independently of operator control to perform their mission. These types of vehicles have been conceived and developed by scientific and military communities over the past few decades, but are now reaching technological maturity as the number of vehicle projects increases and as they begin to enter the commercial arena. At the same time, new technology is becoming available in many areas pertaining to AUV performance, extending their usefulness and mission capabilities [1].

Besides AUVs, underwater missions can be handled by a variety of vehicle types. Among these are manned submersibles, remotely operated vehicles (ROVs) which usually carry a tether that provides power and a communications link, and sensor-equipped sleds towed behind a ship. The existence of these other vehicles lends the AUV to certain types of missions which it is best suited to accomplish, as well as missions which it can accomplish more economically and with a higher degree of safety.

Search and survey missions are one of the most obvious applications for AUVs, taking advantage of the fact that a small AUV can be launched from virtually any platform, can collect data as fast as a survey ship, can be left to its own devices for a period of time, and can be easily deployed as one of a number of AUVs. They can be used to complement manned and ROV missions by completing large surveys, and saving valuable human and ship time for studying only the most interesting areas. Still other uses include providing rapid response to sudden scientific events where a conventionally equipped ship is otherwise unavailable, and providing connectivity and communications between undersea devices [2].

1.2 Defining AUV Performance

Of course, the missions described above necessitate a certain level of performance to achieve their goals. For example, if the AUV's battery can only operate for an hour before needing to be recharged, then many of its advantages are lost. One can define five technological areas that pertain to AUV performance. These are: autonomy, energy, navigation, sensors, and communications [1]. From an even broader standpoint, the better AUV is the one which performs faster, longer, and collects better data than another. Bluefin Robotics points out an interesting link between these three primary areas of performance, pointing out the fact that onboard energy primarily goes to either the propulsion system or the sensors. Following that line of reasoning, a less power-hungry propulsion system will leave more power for the sensors to use and thus result in better data [3]. It is clear that energy is currently the primary limit to AUV performance.

The MIT Sea Grant Autonomous Underwater Vehicle Laboratory operates Odyssey Class AUVs, which have been the subject of ongoing improvements to all of their systems. This thesis will investigate the conventional methods of propulsion currently being used in Odyssey class and other AUVs, and propose a method of implementing promising high-efficiency oscillating foil propulsion technology. Developing new technology to address the propulsion problem will increase AUV autonomy, and widen their practical role in the ocean.

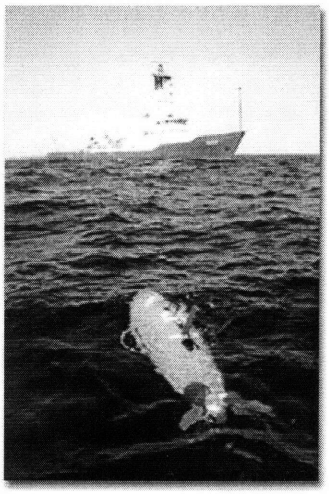

Figure 1: AUV *Xanthos* Odyssey IIb Class returns to the ship [16]

Section 2

Study of the Current Odyssey II Tail Cone Design

2.1 Conventional Propulsion Methods

At present, several types of propulsion systems are commonly used in underwater applications. The first is analogous to an airplane control system and is the same concept used by torpedoes. Thrust is generated by a propeller, and control fins steer pitch and yaw motions by deflecting the flow. This type of system has been widely studied. Propeller-motor combinations can be optimized for efficiency, and when traveling in a straight line with small control surface movements, drag is quite low. Hull shapes for these types of systems are also generally low drag forms to maximize speed and endurance while cruising steadily. At slow speeds, however, there is little flow over the control surfaces and it becomes difficult to maneuver.

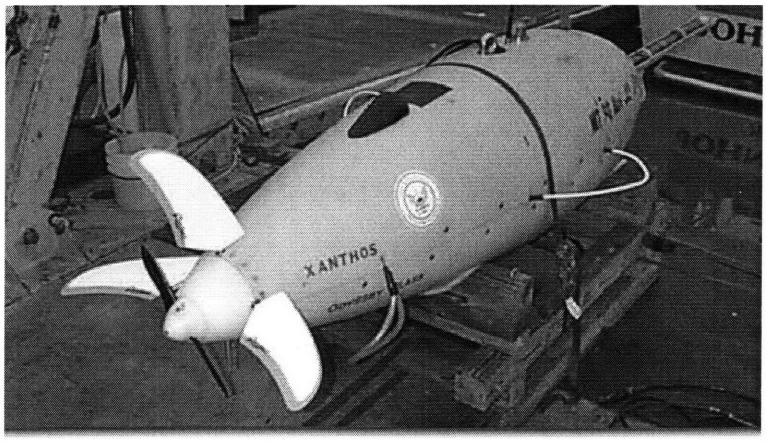

Figure 2: AUV *Xanthos* uses control fins and a propeller [16]

A second type of system uses maneuvering thrusters analogous to those on the space shuttle. These thrusters are located at various points on the vehicle and control all

degrees of freedom. A vehicle that uses this system is likely to be highly maneuverable but at slow speeds. Hence, this approach lends itself to ROVs with cameras and robotic arms. These type of boxy, tethered ROV's don't have the same energy concerns as AUVs if they are powered from the support ship, but the fact remains that thruster based propulsion systems are not suited to higher speeds.

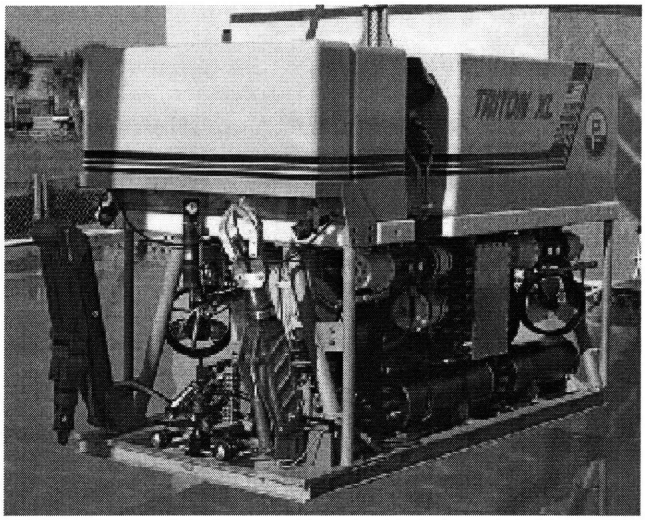

Figure 3: Perry Tritech's Triton XL ROV uses maneuvering thrusters [17]

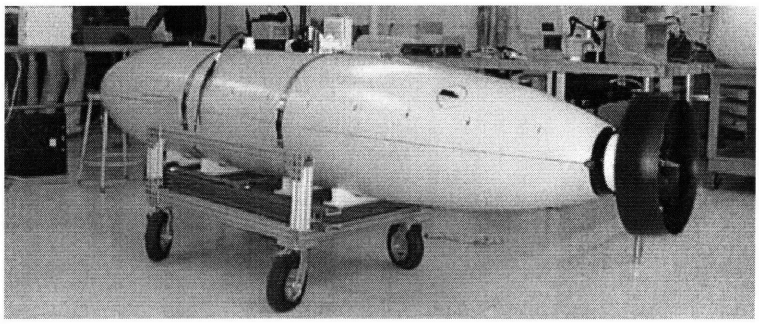

Figure 4: Bluefin Robotics' Odyssey III uses vectored thrust [18]

The final system is somewhat of a compromise between maneuverability and speed, and has found a place on the Odyssey III vehicle. It uses thrust vectoring to steer by angling the ducted propeller vertically and horizontally. No control fins are used so the vehicle can maneuver at low speeds as well as cruise steadily at high speeds.

2.2 Summary of the Odyssey II Tail Cone

The Odyssey II AUV uses a propeller and control surface arrangement, the first type of propulsion system described in section 2.1. The preliminary step in an effort to improve on the Odyssey propulsion systems was to conduct a design review of the present system.

Mechanically, the tail cone mechanism is elegantly simple [Figures 5,6,7]. The housing continues the hydrodynamic shape of the AUV's fairing, with a freely rotating propeller hub on the aft tip. Inside, the hub is connected to a thruster via a bearing supported shaft. Also situated in the housing are the elevator and rudder shafts which pass horizontally and vertically through the housing. Outside the housing, these shafts are fitted with the control fins. One servo unit controls each shaft via a worm-wheel gear train. The output shaft of each servo drives a worm which rotates the wheel mounted to the fin shafts.

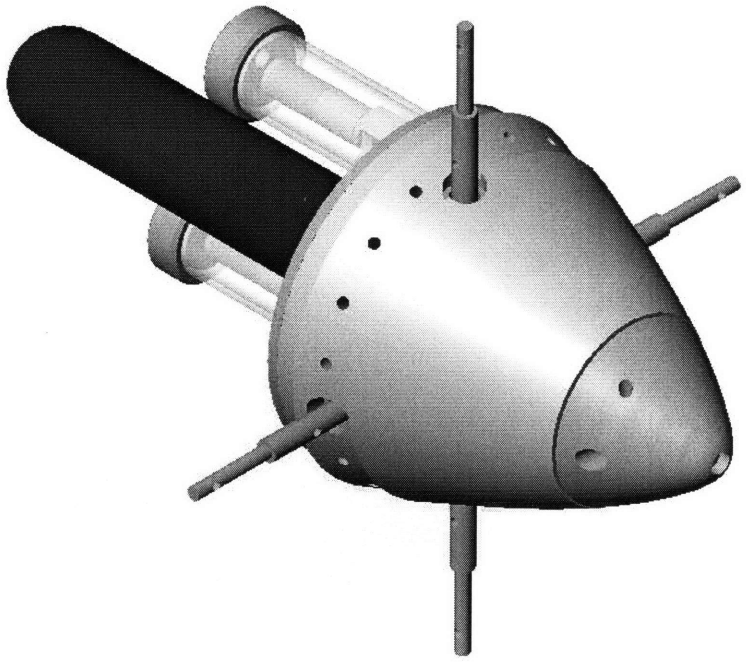

Figure 5: Model of Odyssey II tail cone

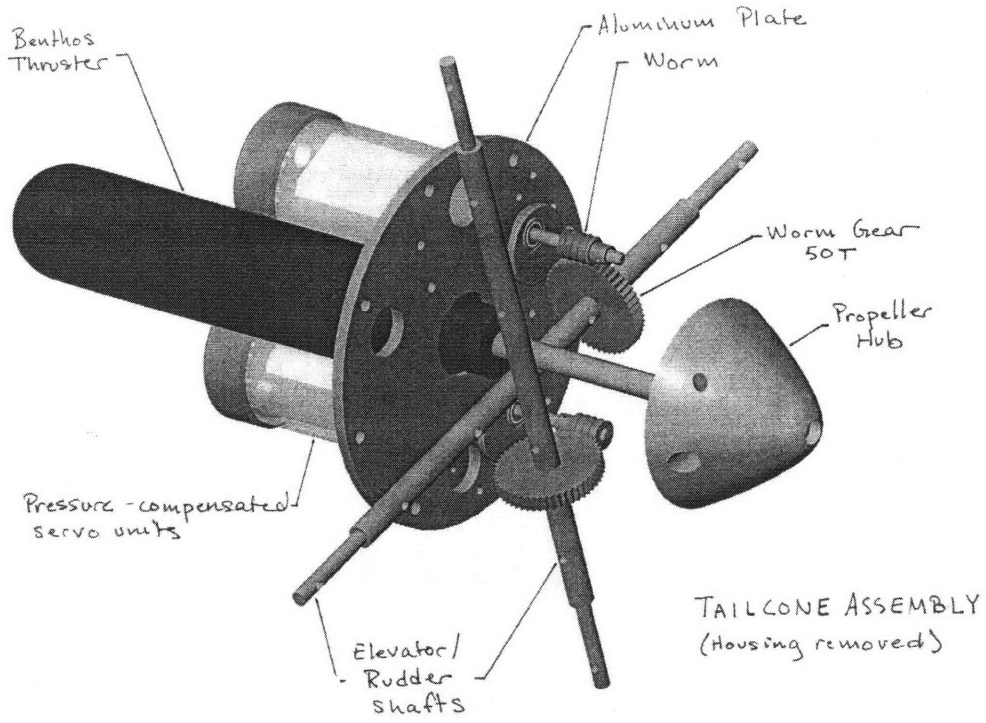

Figure 6: Tail cone assembly with housing removed

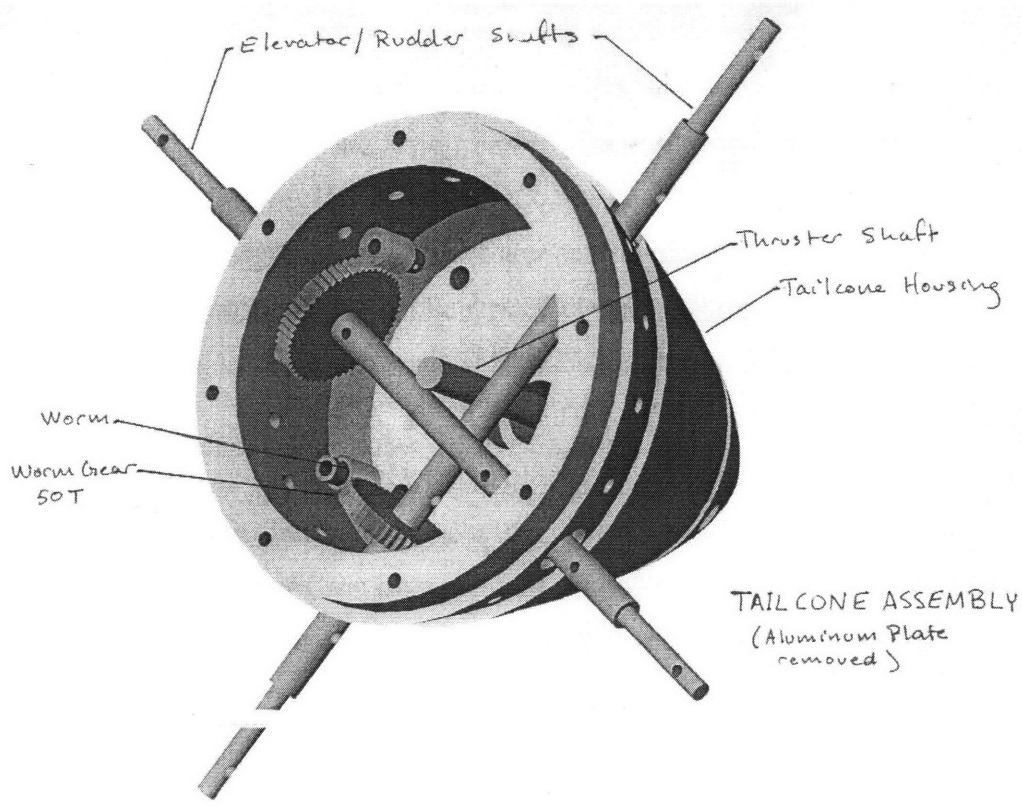

Figure 7: Tail cone assembly with aluminum plate removed

The mechanical system must also succeed in solving three key problems with making the system work underwater. First, and most obviously, the system's water-sensitive components must be shielded from moisture. In order to remain neutrally buoyant and avoid extremely difficult sealing issues, both the Odyssey and its tail cone are free flooding. The thruster is designed for underwater applications and comes from the manufacturer pressure tested to ten thousand psi, or about six thousand meters depth. The other sensitive components, the fin servo units, are housed in a pressure compensated bladder filled with oil. Shaft seals are a potential point of failure for the unit and they were tested to ensure long life under normal operating conditions.

While the motors are safely in their housings, the rest of the mechanism is exposed to seawater. Since seawater is a highly corrosive liquid, materials were chosen carefully to limit its effects. The housing itself is made from polyethylene, a non-corrosive plastic. Vital moving parts like the shafts and worm are made of stainless steel. The worm wheel is made of bronze, a softer metal typically paired with stainless steel worms. Corrosion is evident, but does not significantly affect performance. Indeed, in over five hundred dives, only one worm wheel was replaced.

A control system feedback mechanism has been absent from the design thus far, but is necessary for closed-loop control of the fin positions. The propeller thruster has sensors inside its housing, but to control the fins, a method is needed to sense the true position of the shafts. In the harsh seawater environment, Hall-effect sensors still function. These sensors are small integrated circuits and that sense a change in magnetic field. A ring magnet is fixed to each shaft such that it rotates in close proximity to a Hall sensor mounted in plastic on the aluminum plate. In Figure 8, the sensor chip is mounted in the center of the box. The magnetic field varies as the magnet turns, causing the voltage output of the Hall sensor to change. When the output voltage is compared to a calibrated index of values, the fin's position is known and can be fed back to the servo controller. This system is adequate but somewhat cumbersome, as it requires recalibration when the power to the vehicle is cut off.

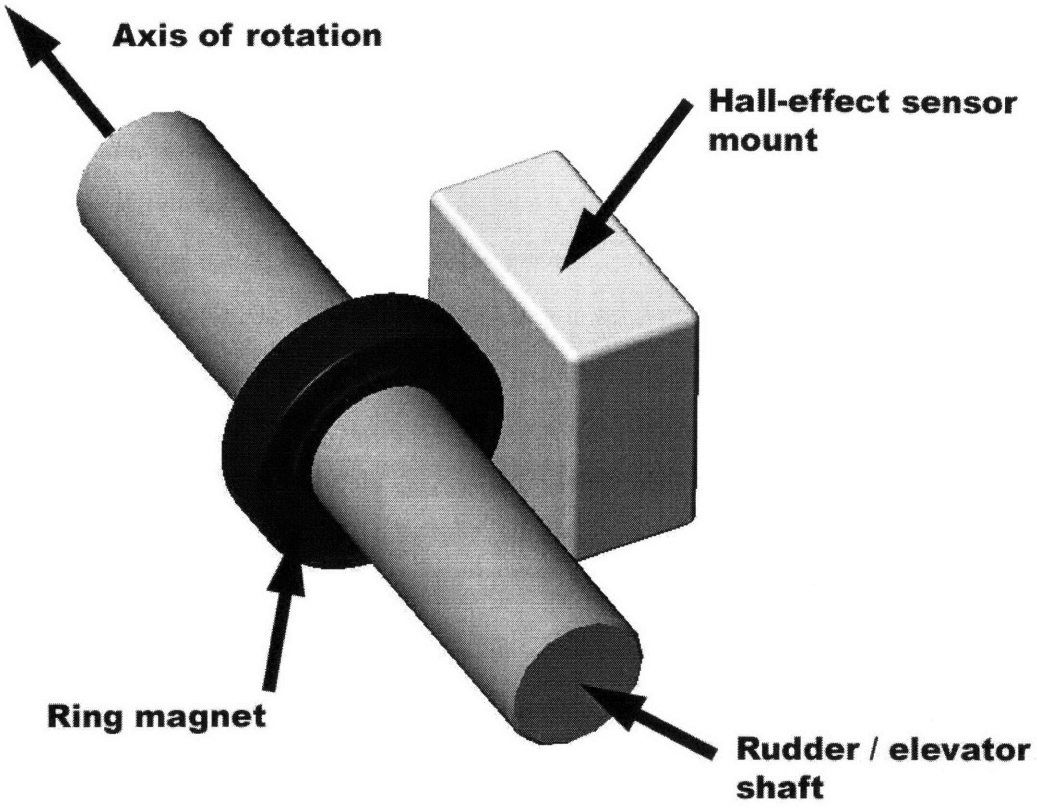

Figure 8: Hall-effect sensor schematic

The Serial ASCII Instrumentation Loop (SAIL) is a serial bus that delivers commands from the AUV computer to the actuator modules. This bus was adopted as a standard by the Institute of Electrical and Electronics Engineers (IEEE) in 1985. The SAIL controller issues commands by raising the attention of one module in the loop, communicating with it, and then releasing it to operate independently until called again. All commands travel through the entire loop but are ignored by irrelevant modules. This system may have been chosen for its resistance to noise and the fact that it can be monitored and debugged easily by plugging a serial terminal anywhere in the loop, however the standard is becoming dated and alternatives should be explored for the future.

Figure 9 shows a conceptual block diagram of the control scheme. In depth documentation of the tail cone and its relevant systems can be found in an annotated

compilation of relevant documentation by the author [4]. The most pressing design issue is the fin servo feedback, which is being investigated by the AUV Lab concurrently with this thesis.

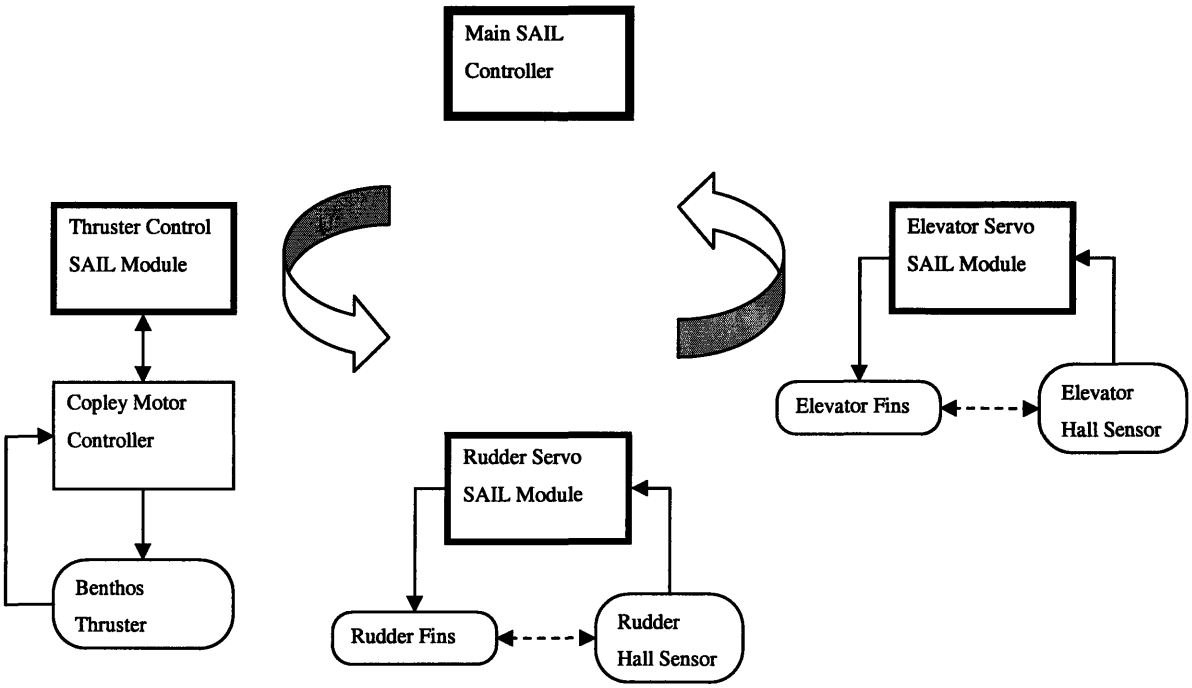

Figure 9: Control system diagram

Section 3

Background on Fish-like Propulsion

3.1 Introduction

Propulsion through the water has centered around the propeller ever since sailing ships lost economic viability a century and a half ago. There are other methods of propulsion using jets and paddles, but the propeller works so easily when simply coupled to a rotating shaft that it has had little competition. Large amounts of research have gone into optimizing the propeller for different applications, including AUV propulsion. Indeed, it is a straightforward design decision to provide thrust for an AUV with a well matched, efficient, propeller-thruster combination. Only recently, when the significant benefits of high propulsive efficiency and maneuverability have become necessary and feasible to implement, have researchers began to seriously consider mimicking nature's swimming machines: fish.

There are many applications for a powerful, maneuverable, long range undersea vehicle. The navy in particular is interested in mine warfare, oceanographic data collection, submarine support, reconnaissance, and operations in turbulent coastal waters where traditional AUVs have trouble operating. Scientific missions can benefit from longer range and the ability to move deftly around an area of interest. In essence, the ability to move like a fish makes it easier for AUVs to accomplish any proposed mission.

Fish have evolved over millions of years into optimized swimmers, though not all fish have been optimized for the same task. There are fish that dart around quickly, fish that cruise, and fish that hover and burrow in sand to hide or eat. There are other swimmers as well, like dolphins and whales, eels, rays, jellyfish, squid, and turtles. Tuna, marine mammals, and sharks are cruising swimmers that are likely candidates for

imitation, and the tuna has been singled out as the subject of a significant amount of propulsive efficiency research.

3.2 Early Research

Some of the earliest work was done with dolphins by James Gray in the 1930s. He did some calculations based on comparisons to human muscle that indicated dolphins had about one tenth the power that should be required to swim. His finding became famous as Gray's Paradox, and inspired research into various possible explanations for drag reduction caused by the fish swimming motion and fish skin.

Later Dewar and Graham became interested in studying the fish swimming motion, and made some scientific observations of tuna by observing them in a water tunnel and taking pictures. Their data quantifies several aspects of fish motion in terms of their body length and is presented here as summarized by Barrett:

- The mean cruising speed was 1-2 body lengths per second
- The maximum cruising speed was 3 body lengths per second
- The maximum burst speed is 27 body lengths per second
- The tail beat frequency (TBF) increases linearly with increasing forward body speed (U)
- There was no observable dependence of caudal amplitude on forward speed
- The caudal joint amplitude was between 0.15 and 0.20 body lengths
- The body wavelength is between 1.23 and 1.31 of body length

This research isolates a few key parameters as important to the swimming motion: the tail beat frequency, the caudal joint (tail fin) amplitude, and the body wavelength [5 and 6].

3.3 Oscillating Foils

An MIT study conducted by Anderson et. al. investigated the efficiency of a thrust producing harmonically oscillating foil [7]. They state that the heaving and pitching of a foil produces thrust by forming a flow downstream of the foil's trailing edge. The flow looks like an unstable jet when averaged in time. At certain frequencies,

the interaction of the jet with the vortices being shed by the foil is amplified, and the maximum efficiency is achieved. In dimensionless form, the frequency is called the Strouhal number, which is defined as

$$St = \frac{f \cdot A}{U} \tag{1}$$

where f is the frequency of oscillation in Hz, A is the peak to peak amplitude of the trailing edge of the foil, and U is the forward speed of the foil. This form of the dimensionless frequency is analogous to the vortex-shedding of bluff bodies. The study concluded with several parameters for optimal production of thrust:

- operation at Strouhal number between 0.25 and 0.40
- large amplitude of heave motion-to-chord ratio (of order one)
- large maximum angle of attack, between 15° and 25°
- a phase angle between heave and pitch (pitch leading heave) of about 75° when the reference point for heave motion is at the one-third chord length from the leading edge.

The maximum efficiency recorded was 87% [7].

3.4 RoboTuna

RoboTuna is a towing tank model of a tuna that was used to experiment with swimming parameters in an attempt to determine optimal motion. At 1.2 meters in length, it was fully articulated and could move according to specified kinematic parameters. Fixed to a towing carriage, it could be pulled through the water at a constant speed. If the tuna applied no net force on the carriage, then it was assumed to be swimming on its own. Minimum energy input while self-propelled was defined as optimal swimming motion. Results showed significant drag reductions when compared to "dead-fish" drag, and that these reductions could be attained even without precise tuning.

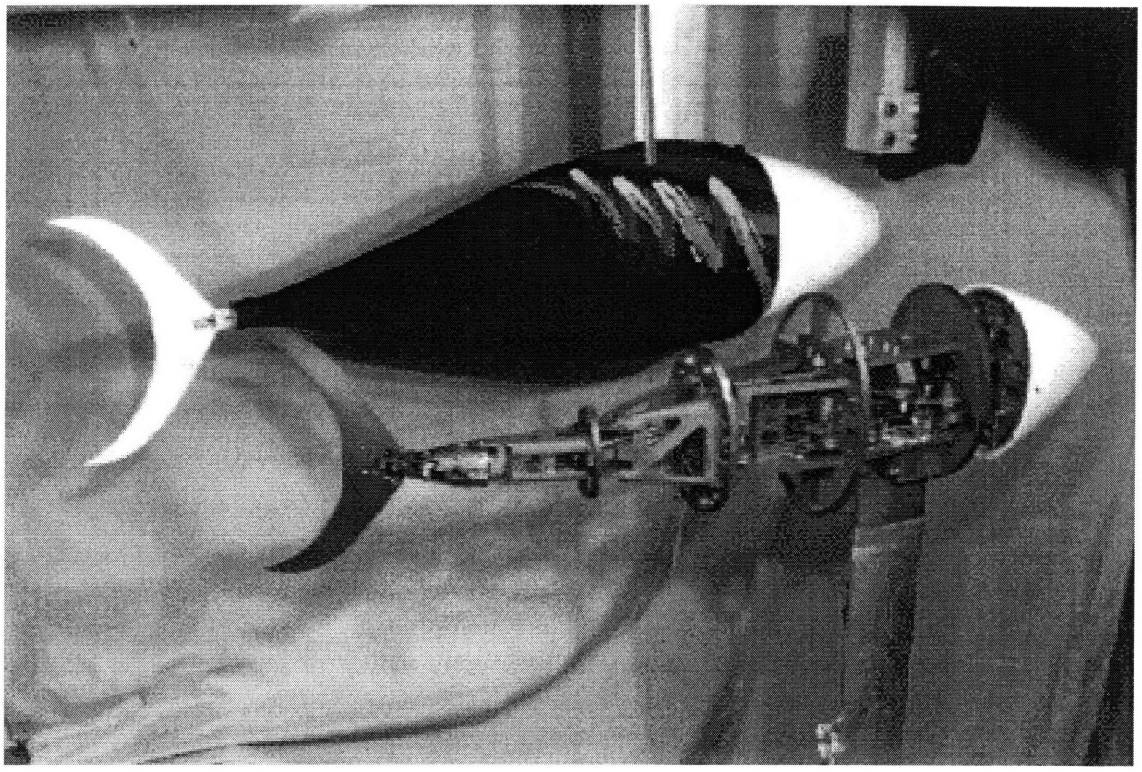

Figure 10: MIT Towing Tank's RoboTuna [19]

Summarized below are the kinematic equations used to model body motion. The y coordinate is lateral deflection, and x corresponds to position along the length of the fish.

$$y(x,t) = a(x)\sin(kx - \omega t) \tag{2}$$

$$a(x) = c_1 x + c_2 x^2 \tag{3}$$

$$\theta_{tail}(t) = \theta_o \sin(\omega t + \varphi) \tag{4}$$

The optimum motion parameters determined by Barrett are summarized in Table 1.

Table 1: Self Propelled Optimum Motion Parameters Derived by Barrett

Variable	Description	Value
U	Swimming Speed in body lengths per second	0.65 L/s *
St	Strouhal Number $= \frac{fA_{TIP}}{U}$	0.156
A_{TIP}	Peak to peak amplitude of caudal fin tip in body lengths	0.115 L
α	Maximum angle of attack of caudal fin during swimming cycle	16.2°
φ	Phase lead of caudal fin motion with respect to lateral body motion	95°
λ	Propulsive wavelength in body lengths	1.27 L
c_1	Coefficient of linear term	0.00372
c_2L	Coefficient of quadratic term	0.203

* Body length L is the distance from the nose to the front of the tail fin [6 and 8]

3.5 Vorticity Control Unmanned Undersea Vehicle

The Vorticity Control Unmanned Undersea Vehicle (VCUUV) was a project undertaken by Draper Laboratories to design, build, and test a mission-scale vehicle that uses vorticity control. Modeled after a yellowfin tuna, this vehicle is 8 feet long and displaces approximately 300 pounds. In testing it has achieved a speed of 2.4 knots and turning rates of up to 75 degrees per second [9].

VCUUV was designed from scratch to demonstrate oscillating foil propulsion in a testing environment of less than 10 meters in depth. Its hull shape was scaled directly from a real tuna, as was its caudal fin. The forward section is pressurized and houses the electronics, batteries, and the hydraulic power unit. The tail section is flooded and is actuated by four hydraulic cylinders. The flexible hull is created through a system of ribs

and splines that make a smooth curve out of the tail linkage, and a layer of overlapping scales prevents folding. Depth control was implemented with two "pectoral fins" that act as dive planes. Placed slightly forward of the vehicle's center of gravity, they imitate the shape and size of tuna fins as a swept and tapered NACA 0015 foil [9].

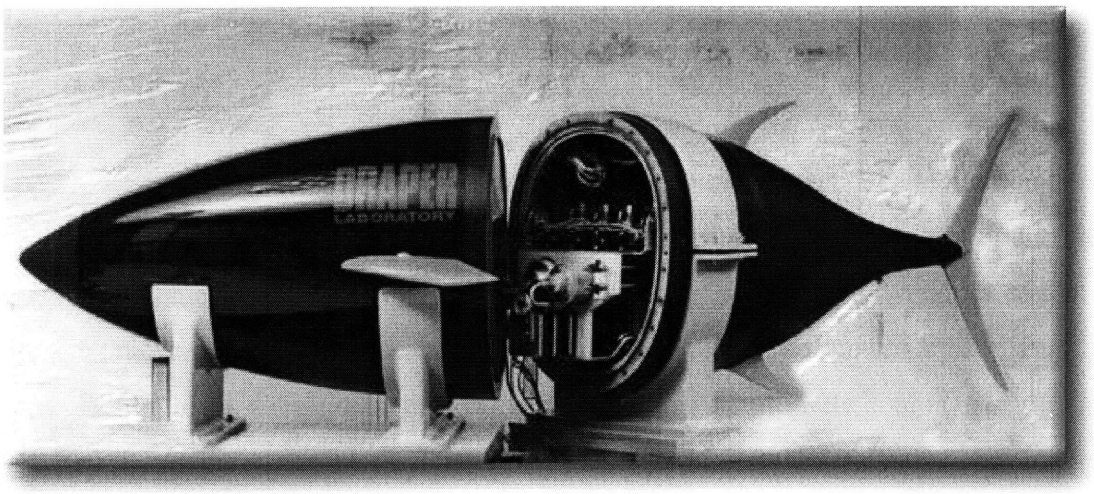

Figure 11: Draper Laboratory's VCUUV [20]

VCUUV based its swimming parameters largely on RoboTuna's determined optimum motion, but designed the vehicle to move at speeds closer to biological speeds of 1.0 BL/s. In practice, however, forces at tail oscillations above 1 Hz were higher than expected and degraded performance. The 2.4 knot maximum forward speed corresponds to 0.61 BL/s, which is marginally slower than RoboTuna's achievement of 0.65 BL/s [9].

Section 4

Design Motivation and Requirements

4.1 Motivation

A significant amount of fish biomimetic research of the past decade has been focused toward modeling and implementing fish-like motion as closely as possible. This is due to the immense number of unknowns and the complicated fluid dynamics of the swimming motion. The "safe" design approach is to avoid the unknowns by copying nature. While this is a legitimate and valuable first step, the ultimate goal is to implement biomimetic concepts in useful, payload-carrying underwater vehicles.

With several proof of concept prototypes in operation, including MIT's RoboTuna and Draper Laboratory's VCUUV, the next step is to stretch some of nature's forms into a practical design and observe how these concessions affect performance. The role of the MIT Sea Grant AUV Laboratory coincides with such practical design goals, by making lab technology field-worthy and deployable for real applications.

The AUV Lab's proven workhorse has been the Odyssey II class AUV. By retrofitting this AUV with a flapping foil propulsion system, important knowledge will be gained about the feasibility of fish-like propulsion for the near future. Since many of the AUVs already in existence are torpedo shaped, success would mean that the technology is broadly applicable to the current fleet without total redesign efforts. This approach suggests the possibility of future modular flapping foil units that could be selected based on vehicle specifications and geometries, much like a propeller is selected.

4.2 Requirements

The practicality of the retrofit concept comes from the acknowledgement that AUVs have many other important systems, without which the cost of launching the

vehicle cannot be justified with any return. These other systems compete for space and electrical power with the propulsion system. They include sonars, cameras, other payloads, computers, batteries, and various pressure housings without which the vehicles depth range would be small. As opposed to a proof-of-concept design, a retrofit acknowledges that these other systems must exist in a real AUV, and works around them for a much lower cost than a new vehicle.

The first retrofit design should attempt to minimize impact on the Odyssey's existing parameters: size, depth rating, stability, operating temperature range, and speed. The ultimate goal is a benefit in efficiency and maneuverability, not necessarily a change in performance parameters, although that should be the end result as the technology develops. However, in order to prove the retrofit concept, power consumption and efficiency will be temporarily subjected to the need for a working prototype. As discussed previously, one of the reasons for imitating nature is to bypass complex mechanisms that are difficult to model. Maneuverability is even more complicated to address than the steady swimming motion because fish use a multitude of fins for control, not just a caudal fin. Again, the retrofit should concentrate on the steady swimming motion and not on mimicking the subtle details of maneuvering and depth control, although those requirements should be investigated. In short, the implementation of a flapping foil system should strive to minimize impact on the vehicle and increase maneuverability, but can count on future modifications to increase its performance to theoretical values.

As opposed to a testing tank vehicle, the Odyssey retrofit needs to be robust and compatible with the vehicle's typical missions. It may sustain a hard knock, or saltwater corrosion, and it must be serviceable aboard a ship. With larger moving parts under stressful cyclical loading, component lifetime becomes a serious issue. Similar to a testing tank vehicle, the mechanical system design should have room to adjust its swimming parameters to account for differences between previously studied geometries and the new shape. The system should be operable within these broad parameters by the control system, which is not within the scope of this thesis.

Section 5

Concept Definition and Design Evolution

5.1 Early Decisions

Approaching this design problem was not starting from a clean slate, but examining the results of past experiments, observations, and vehicles. From there, it was necessary to decide which features were the most important, which parts should conform to nature, and which could be changed in order to accommodate a retrofit design. Throughout the process an attempt was made to brainstorm, think broadly and explore many options.

As discussed earlier, the new propulsion system is designed to demonstrate steady forward swimming. By removing the old tail cone, all elements of yaw, pitch, and roll control have disappeared and must be replaced by new systems. Yaw control could conceivably be accomplished with the flapping tail fin itself. Instead of continuing its flapping motion, the tail would move to the extreme limit of its travel and act like a boat rudder to control yaw. It is also conceivable that Anderson's average jet flow could induce a slow turn by flapping the tail off center to one side [7]. Pitch is not controllable through the tail, and mimicking a second type of fish fin would be irrelevant to the primary concept. A conventional substitute is to add diving plane control surfaces. Since they can no longer be located on the tail cone section, it makes sense to place them forward where a fish's pectoral fins are located. They can be actuated from inside the AUV with the current control fin servo actuators. Both the port and starboard actuators would be synchronized so that differences in their angle do not cause strange yaw and roll effects. On the other hand, if the dive planes operated independently, they could potentially compensate for unforeseen yaw and roll effects from the tail. To minimize

roll, fixed stabilizing fins should be added much as they appear on a tuna, in the dorsal and anal locations.

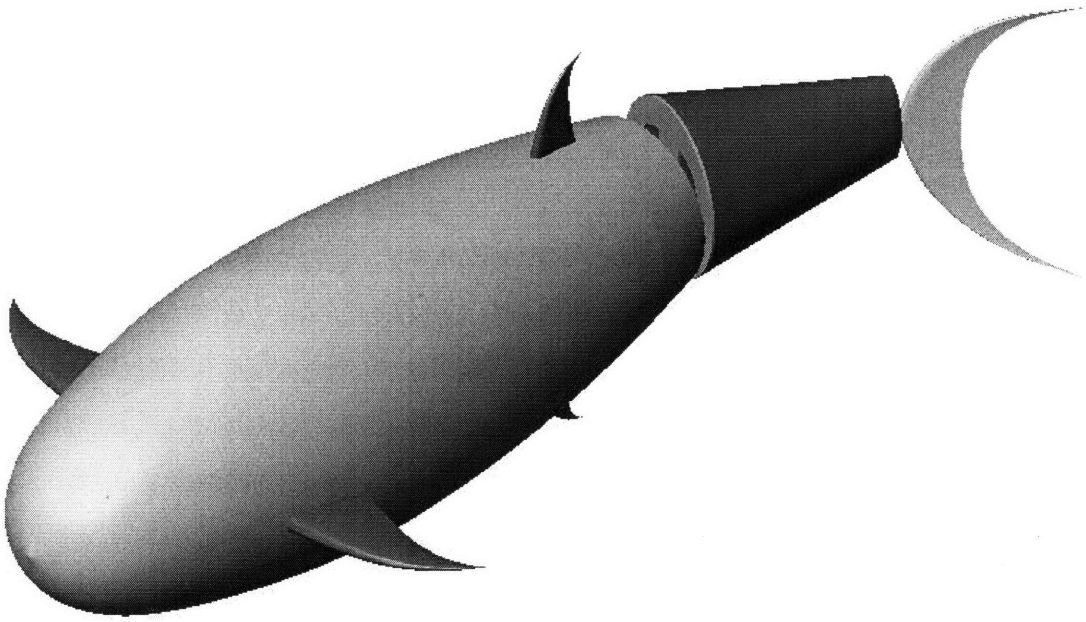

Figure 12: Concept model for the Odyssey flapping foil retrofit

The after section of the Odyssey II is defined by two posts that hold the top and bottom of the fairing together, as shown in Figure 13. These posts are located just aft of the battery sphere. With the conventional tail cone, the distance from the posts to the propeller is 24 in. The external diameter of the fairing at the posts is 17 in.

Any given section of an AUV can be either watertight or free-flooding. The Odyssey II is rated to 3000 meters depth and has a +0.5 kg buoyancy, indicating that it has a slight tendency to float to the surface. These traits are accomplished in part with a freely flooding body. Dry components are contained in pressure spheres which can more easily withstand deep depth than complicated geometries such as sections of a fish tail. Additionally, when the body is flooded, neutral buoyancy is more easily achieved. In

order to maintain deep depth capability and leave the vehicle's center of buoyancy relatively unchanged, the tail section should be flooded. However, the water inside the vehicle should move with the rest of the tail and not flow across the "skin" if the integrity of the external flow is to be preserved.

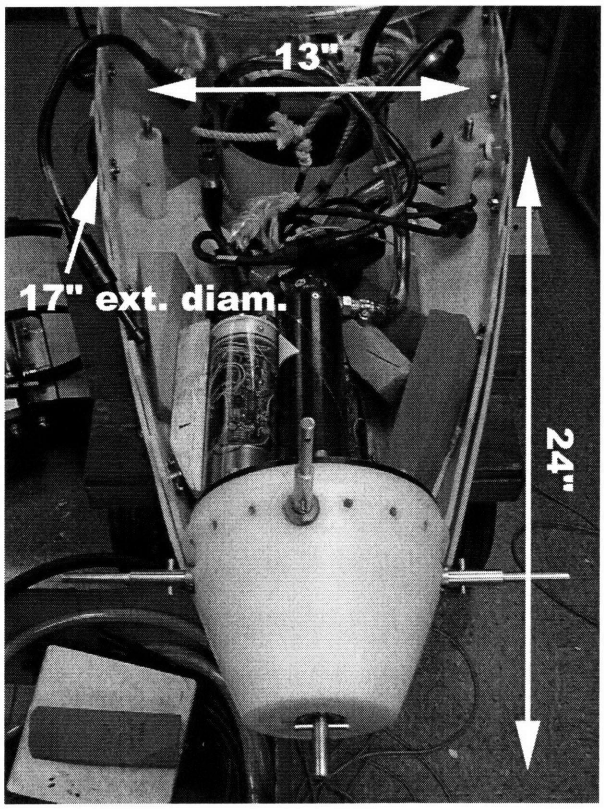

Figure 13: Photo of Odyssey tail cone dimensions

At this point in the design the next step was unclear. Several decisions needed to be made, including the geometry of motion, the number of joints, the method of actuation, and the method of enclosing the entire assembly into a smooth, impermeable shape. Each choice was thoroughly intertwined with the others, and many potential designs were contemplated to oscillate a fish tail and caudal fin. Possibilities included single rigid links, vertebrae, ribs, flexible battens, dual backbones, gears, tendons, springs, magnets, rotating sections, scales, stretchy skins and more. At this point, it seemed that the design would be inextricably linked to its method of actuation. This approach may have turned out a working novel design eventually, but the need to make

progress within one semester dictated a different approach. The actuator question was dropped for the moment, in favor of reexamining the geometric requirements of swimming and developing a better model of the system dynamics.

5.2 Designing the Swimming Motion

As a starting point, the decision was made to use two links, a rigid main tail link and an independent caudal fin. The following are the reasons. First, simplicity is the key to a robust design that is limited in size and in terms of power required. Further, it is not known how the Odyssey's geometry will perform hydrodynamically. Interestingly enough, it is known that salmon can generate substantial thrust even without their caudal fins [13]. This phenomenon substantiates the fact that by not copying the tuna exactly, there is less certainty that the vehicle will perform near optimally. However, negative effects are expected to be reasonable. The Odyssey is a low drag, hydrodynamic shape. Although it is wider in the body than a tuna, if the tail section gradually flattens and tapers like a tuna's, some of the hydrodynamics will be similar. A fully articulated tail may be more complex than it is worth, given the other hydrodynamic vagaries in the system. The caudal fin, on the other hand, has been studied and characterized as a thrust producing element. The importance assigned to phase and angle of attack by Anderson, et al. has been demonstrated, and it is known how to optimize the foil's parameters [7]. Added complexity is justified in the independent caudal fin because it moves out of phase with the rest of the body, and it is known that substantial thrust can be generated with proper motion.

Prior studies have indicated several parameters that lead to optimum swimming configurations. The body length is the unit by which all the parameters are measured, and is the length from the nose to the beginning of the caudal fin. To minimize impact on the Odyssey, its length should not be extended to more than 95 in. from its original 87 in. This does not include the caudal fin, which will add even more length. Once the body length has been set, a design speed should be set. A reasonable maximum design speed is that of RoboTuna, 0.65 BL/s or about 1.5 m/s, as efficiencies are likely to be lower in a less optimized system. The Strouhal number should be set at 0.25 and the peak to peak

caudal amplitude at 0.15 BL, which are consistent values with biological observations. RoboTuna's optimum values are lower and may be used during operation, but the more demanding biological values should be used for design so that the system has extra capability. With those parameters defined, the Strouhal relationship (Eqn. 1) dictates that the necessary tail beat frequency is around 1 Hz.

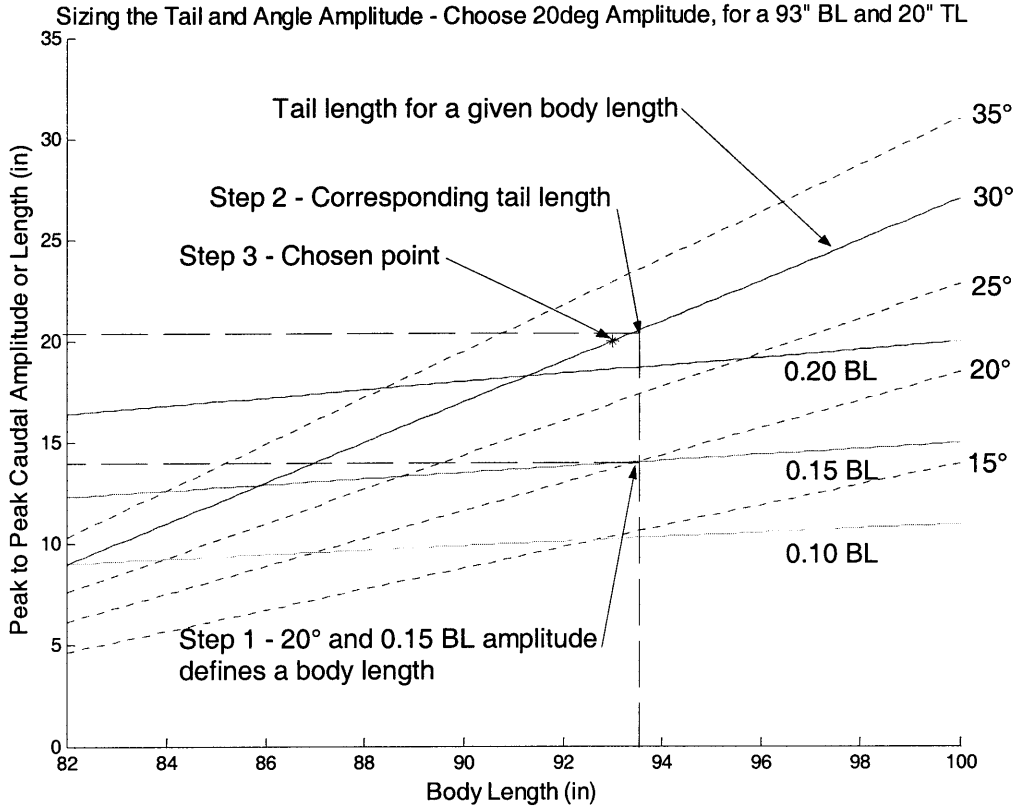

Figure 14: Sizing scheme for body and tail length

Figure 14 represents the scheme devised for choosing an overall body and tail length. Each solid line represents a percentage of the body length corresponding to peak-to-peak caudal amplitude. The lowest line represents 0.10*BL, the middle 0.15*BL, and the top 0.20*BL. The diagonal solid line represents the movable tail length, which is determined by subtracting the fixed length from the overall body length. Each dotted line represents the amplitude achieved by a given tail angle. The lowest dotted line corresponds to 15° and higher ones increment by 5°. The result is that a low 20° tail

angle can be achieved within the body length range, while also achieving the 0.15*BL amplitude goal. The corresponding tail length is 20 in. [Appendix A].

5.3 Modeling the System

With the available information on the tail's likely geometry and motion, the next step was to estimate the forces required to move the tail through the water. The approach was to assume a sinusoidal motion and predict the torque required to directly drive the tail. A computer model was created in MATLAB® to ease manipulation of the parameters according to design changes and changes in desired swimming parameters. The complete script can be found in Appendix B.

The model uses the following parameters as a basis for all its calculations: body length (BL), tail length (TL), design velocity (U), Strouhal number (St), and amplitude (A). The Strouhal number relationship, then fixes the necessary tail beat frequency (TBF) in Hz to achieve the design speed.

$$TBF = \frac{St \cdot U}{A} \tag{5}$$

According to Dewar and Graham, the TBF scales linearly with forward velocity, while the amplitude does not affect it [5]. This indicates that once an amplitude parameter is chosen it should be treated as a constant, while TBF is varied to control speed.

Two main forces act on the oscillating tail, forces to inertia and forces due to drag. It is assumed that the angle of oscillation will be small enough that drag forces will be primarily due to lateral motion and will not be significantly affected by the vehicle's forward speed. This assumption may merit further consideration. The tail is discretized into four cylindrical sections of constant diameter for simplicity and to build a factor of safety into the force estimates [Figure 15].

For the inertia calculations, each section has an elliptical cross-section and is treated as a point mass at its geometrical center. The tail is determined to be neutrally buoyant and therefore each section's density must average to the density of seawater. As an extra factor of safety and to account for added mass moved by the tail, the calculated

mass is augmented by a factor of 30%. The moving mass of the caudal fin also exerts force on the very tip of the tail, and its mass is estimated based on the density of fiberglass. Finally, each mass is converted into a moment of inertia based on its distance from the center of rotation, and summed to yield an equivalent moment of inertia for the entire tail. The torque on the system is the equivalent moment of inertia times the sinusoidal angular acceleration.

For the drag calculations, each section is approximated to be a cylinder in cross flow in order to determine a reasonable drag coefficient. Flow is characterized by the Reynolds number, which is proportional to the density of the fluid ρ, the velocity of the fluid, v, a characteristic diameter, D, and inversely proportional to the viscosity, μ.

$$\mathrm{Re} = \frac{\rho v D}{\mu} \tag{6}$$

For a cylinder in water moving at speeds corresponding to a 1 Hz flapping motion, the Reynolds number is on the order of 10^5. Based on well known experimental data, this corresponds to a conservative drag coefficient of 0.4. The following equation is used to determine the drag force on each segment:

$$F = \frac{1}{2} C_D \rho A v^2 \tag{7}$$

where F is the force exerted, C_D is the coefficient of drag, ρ is the density of water, A is the projected area in the flow, and v is the velocity [10]. To account for the caudal fin, an approximate projected area is estimated, and the coefficient of drag for a flat plate, about 1.0, is used in equation 7. The force on each section is then converted into a torque based on its distance from the center of rotation, and then summed into an equivalent torque on the system.

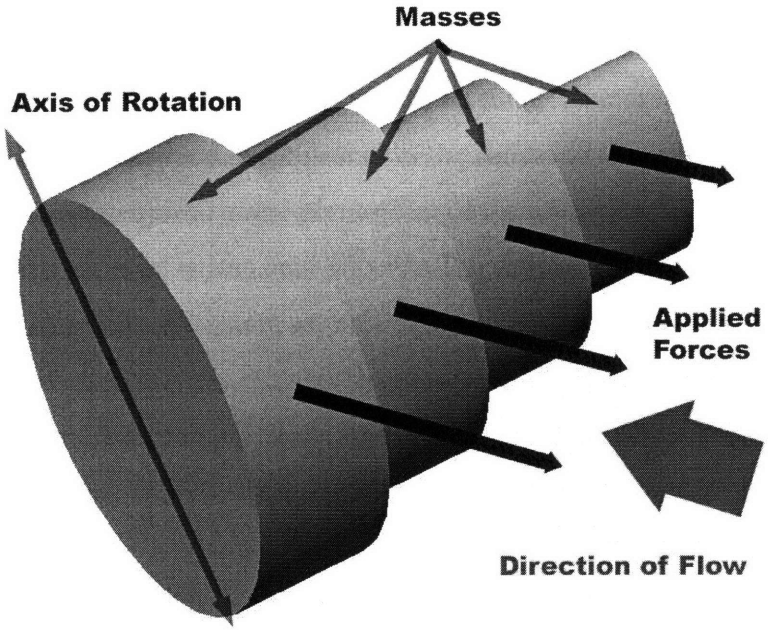

Figure 15: Sketch of model elements

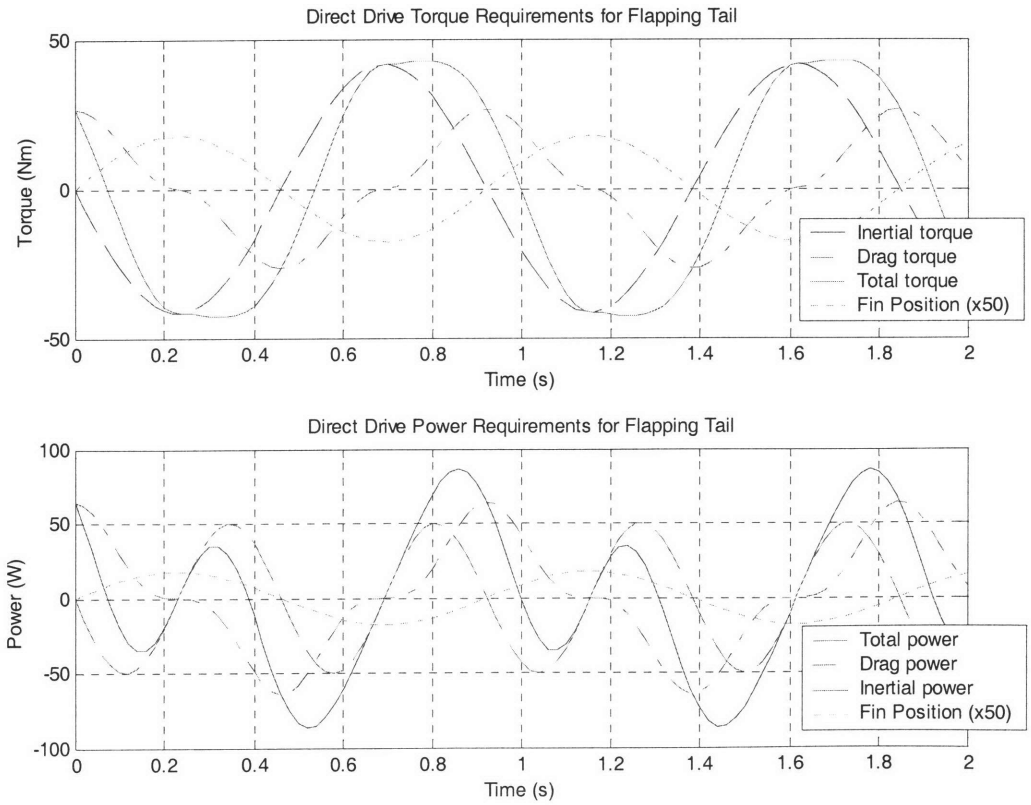

Figure 16: Required torque and power model for main link

Figure 16 shows the output of the MATLAB® script when the required torques are plotted individually and when they are summed linearly. Instantaneous power is calculated as the instantaneous torque times the velocity. The drag terms are periodic but not sinusoidal because they are proportional to the square of the velocity of the fluid. The maximum torque required at the pivot point of the tail is less than 50 Nm, and the mechanical power required is less than 100 W. The set of calculations has been done for steady state motion with parameters as discussed above. It should be noted that increasing the TBF, and thereby the vehicle speed, has the greatest effect on the maximum numbers. Additionally, the hydrodynamic forces due to vehicle forward motion tend to increase the forces on the lateral tail motion as speed increases. The model has made conservative estimates in order to build in a factor of safety, and has neglected the effects of forward motion in this model. If higher TBFs are attempted, these forces may have a significant effect.

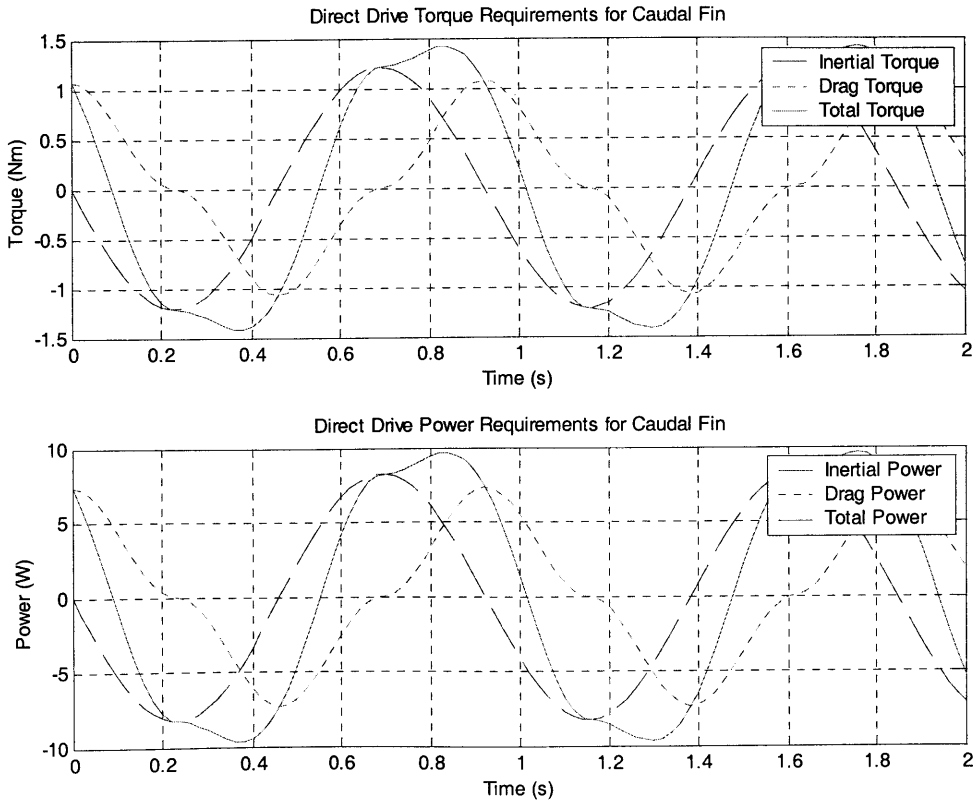

Figure 17: Required torque and power for the caudal fin

The same procedure was applied to the caudal fin joint [Figure 17]. The caudal fin joint is less massive, shorter, and only needs to drive itself. The model was conducted using a caudal fin center of mass 18 cm from the caudal hinge [Appendix C]. Torque and power requirements are much lower at 1.5 Nm peak torque and about 10 W peak power.

5.4 Actuator Study

There are many types of actuators currently available to designers. Three overall guidelines were observed when investigating the wide variety of choices. First, and most obviously, the mechanical, electrical, and space requirements of the design must be met and preferably exceeded. Second, the AUV Lab subscribes to the current trend of using commercial off-the-shelf components as a way of reducing cost, facilitating repair and replacement, and saving design time in favor of implementation and testing time. Third, no type of actuator was dismissed without at least a preliminary look.

Hydraulic actuators were initially a very attractive choice, a fact confirmed by their use in VCUUV and future concept designs done by Barrett [11]. Hydraulic cylinders can push and pull in a compact package, and deliver high forces. Hydraulic servo valves are commercially available to electronically regulate cylinder speed and position. Parker Hydraulics, among others, makes a hydraulic power unit that contains everything but the servo valves and cylinders. Feedback would not be difficult to incorporate. Additionally, the hydraulic pump would run at a constant, optimized speed to efficiently maintain pressure in the system. Unfortunately, there are also many drawbacks to hydraulics. The system is inherently complicated even with the all-in-one power unit, and there are opportunities for leaks. Pressurized hoses will be connecting all the parts, and the fatigue of an oscillating motion could be an issue. The system would be fairly large and heavy, and although it might be possible to package it within the tail as is, it is obvious that the unit is designed to run in air. Pressure compensation packages, even if feasible, would probably make the unit too large. There is simply not enough freedom in a retrofit design for hydraulics.

DC linear actuators are an electrical alternative to hydraulics. Currently the Odyssey III uses a custom linear actuator to provide vectored thrust for its ducted

propeller. These actuators usually consist of a DC motor driving an Acme or ball screw that causes smooth extension of a rod. They are usually characterized by an extension speed, a maximum force, a stroke length, and a duty cycle rating. Usually the ball screw designs are rated for 100% duty cycle, which means they can be used continuously. Linear actuators can be pressure compensated, but may be prohibitively long. However, shorter stroke lengths and lower force requirements result in smaller sized actuators that may be suitable for use with the caudal fin.

In the field of biomimetics, it may eventually make sense to mimic muscles as a method of actuation. Shape memory alloys are a developing technology that promises to be used in these types of applications. There are many types of these actuators, but the simplest type may be the strand of NiTi wire that contracts to a predetermined shape when heated by electrical current. Water even seems like an ideal medium to use the wires since it would cool the wire rapidly, facilitating temperature control. Unfortunately, along with piezoelectrics, these actuators would require prohibitively high voltages, and are not feasible for AUV design at this point in time.

Finally, perhaps the most common electromechanical actuator is the DC motor, which comes in thousands of varieties. There are brushed and brushless servo motors, stepper motors, gear motors, and others, each type requiring electronics in order to control. A likely best choice is the brushless servo motor, which uses electronic commutation to reduce motor size, prevent brush failure, and reduce noise. DC motors can be characterized by a host of numbers, most notably the torque-speed curve and various electrical characteristics. In general, motors function poorly under oscillating loads, drawing high currents when reversing direction, and operating efficiently at a single torque and speed, not at a constant ramp up and ramp down. Linkages may be used to eliminate the motor reversal problem, but sacrifice the compact design, incur frictional losses, and do not necessarily eliminate the efficiency problem.

Nevertheless, motors are compact and can take advantage of many transmission systems designed to exploit their use. Cables and pulleys were used in RoboTuna to design a low backlash system that allowed flexibility in choosing a transmission ratio. A servomotor drives a winch that simultaneously pulls in the cable on one side and lets it out on the other side, reducing backlash. Nylon coated wire and plastic race pulley

bearings are available to hamper the effects of corrosion and decrease mechanical losses. Pulleys and winches must be of large enough diameter to allow the cable a long life. This type of system relies heavily on preloading the cable to avoid slip. This design was initially very attractive because it made motor selection much easier through its versatility. Unfortunately maintenance concerns discarded this idea. It is interesting to note that a while after RoboTuna's initial experiments, extra compliance and friction in the transmission prevented the repetition of RoboTuna's excellent results [12].

An alternative to pulleys is a cable chain drive. These are made of polyurethane coated cables that fit around anodized sprockets, resisting corrosion. These systems are inherently no-slip, and do not need as large a preload as the pulleys. The sprockets face the same bearing friction problems as pulleys, but there are fewer sprockets, minimizing frictional losses. Chain drives transmit rotary motion to rotary motion and do not have the same potential as pulleys for high transmission ratios. A chain drive system would likely be a direct drive mechanism, requiring a high torque, low speed motor and high strength chain.

5.5 Summary

Several key decisions were made as the Odyssey retrofit concept developed. The design was approached with the intent of minimizing impact on the existing Odyssey design and concentrating effort on the tail fin swimming motion. Provisions were made, however, for pitch-controlling dive planes in the position of a pectoral fin in the forward section of the vehicle. Based largely on RoboTuna's self-propelled optimum motion parameters and the Strouhal relationship, the target design speed was set at 0.65 body lengths per second or 1.5 m/s which corresponds to a tail frequency of about 1.0 Hz. A rough model was developed to estimate the torques and power required to move a tail through the water at these speeds. The loads on the main link were the primary concern, needing 50 Nm of peak torque and slightly less than 100 W of peak power about the hinge, while the torque loads on the caudal fin link were minor by comparison. Next, the possible actuator choices were examined for suitability to the application. Most notably, hydraulic actuators were deemed complex and bulky, while the most promising actuation methods were high torque motors and DC linear actuators.

Section 6

Design Proposal

6.1 Introduction

The following section draws on the background research, goals, requirements, and concepts generated in previous sections, and proposes an informed solution in medium detail. The intent is not to present a final design down to the nuts and bolts, but to suggest a feasible design for future consideration. Every effort has been made to address the critical choices involved: structure and space issues, the actuator choice, the drive mechanism, and the flexible skin, while being mindful of essential details such as attachment methods, material choice, and ease of construction.

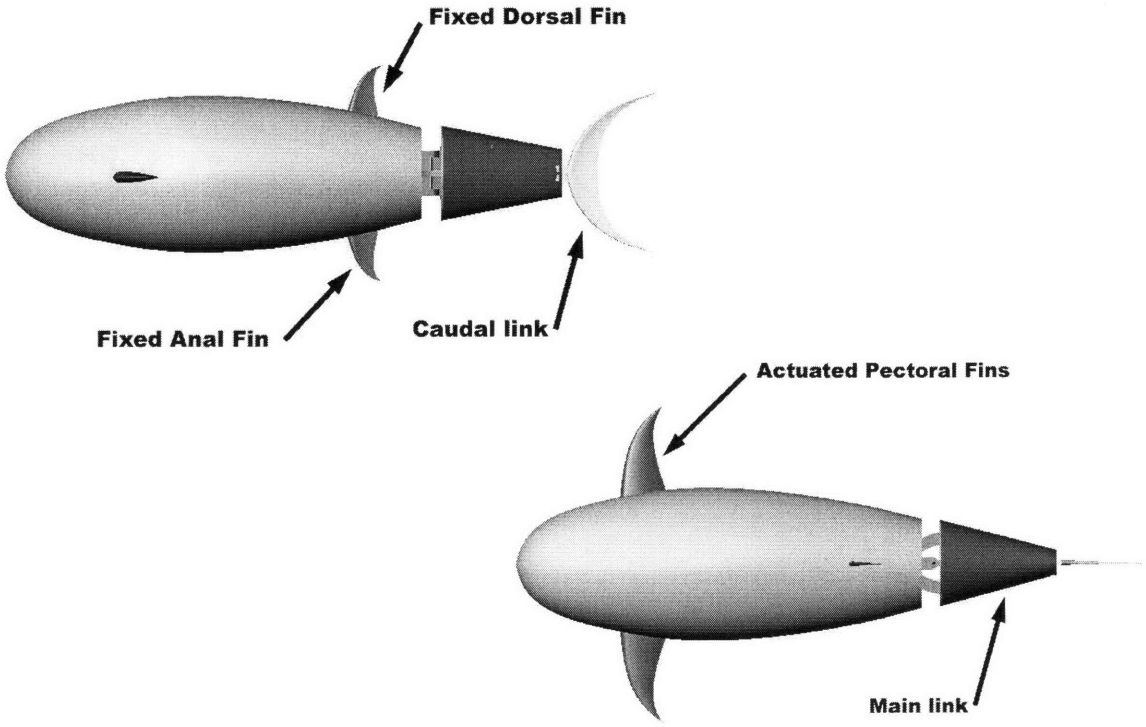

Figure 18: Profile (left) and plan (right) views of proposed design

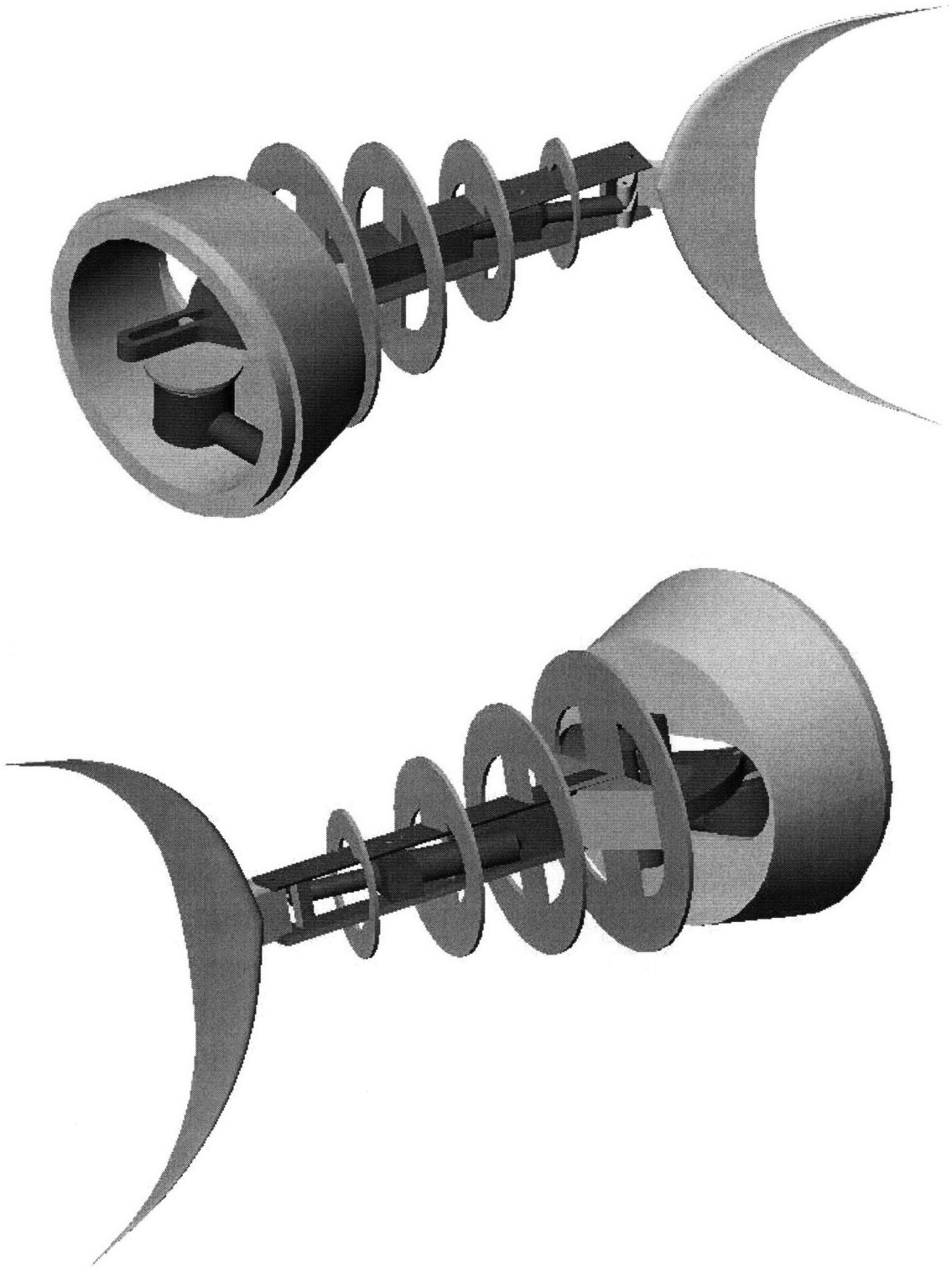

Figure 19: Views of tail assembly skeleton

6.2 Link Structure

Having decided that the articulated tail will consist of one main link and one caudal fin link, the details of the shape and joints need to be chosen. The anatomy of a fish is a guide to the necessary structure and geometry. The shape of the hull should be phased gradually from a circular cross section to a flatter, elliptical section that decreases drastically in area by the caudal fin. The rigid fairing should transition smoothly into the flexible segment, which will be shaped by rib-like bulkheads. The weight of the structure can be offset by attaching foam to the bulkheads in the dead spaces until neutral buoyancy is achieved.

The internal structure of the tail section aims to be flexible in the lateral direction, but stiff in the vertical direction. To accommodate the new tail section, the existing Odyssey fairing will have to be cut off immediately aft of the sphere and posts. The actuation mechanism for the main link will be housed in a near-neutrally buoyant polyethylene housing that can be bolted rigidly to the fairing.

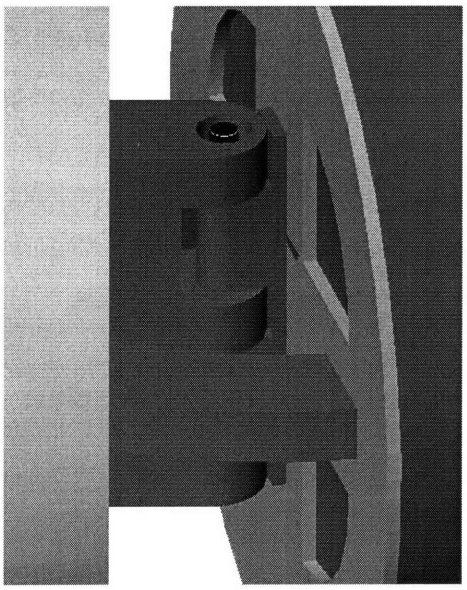

Figure 20: Hinge joint concept

Bolted on the rear side of the housing is the hinge joint for the main link. Friction in the hinge is a significant concern, therefore as large and free a hinge as possible is

essential. A likely case for the maximum load on the tail is the full water-filled weight of the vehicle in air. The hinge will not be stressed underwater if the tail is neutrally buoyant, but if the vehicle comes out of the water quickly, the hinge should be able to withstand the load while the vehicle drains. The torque at the hinge joint for this case is 145 Nm. The hinge shaft should be as substantial as possible and still maintain a high length to diameter ratio and fit in the space. Based on space available, a half inch diameter shaft and a six inch hinge have been selected as a preliminary design.

Since friction will reduce the vehicle's effective power output, bearings should be considered for the hinge. Many new bearing technologies focusing on corrosion resistance are available. For a six inch tall hinge supported at the top and bottom, a bearing would face a 430 pound radial load at our worst case scenario, not under normal operating conditions. Plastic bearings, stainless steel bearings, and ceramic bearings all offer varying load capacities and corrosion resistance. Solid lubricants are also available. Based on loading requirements, ceramic bearings look the most promising. Adequate space has been allotted for thrust and radial bearing mounting on the fixed side of the hinge. On the other hand, if care is taken with the tail, a low-corrosion plain bearing can be made with replaceable Delrin bushings, and may prove adequate. Friction and corrosion effects in different bearings should be experimented with further to better characterize the system.

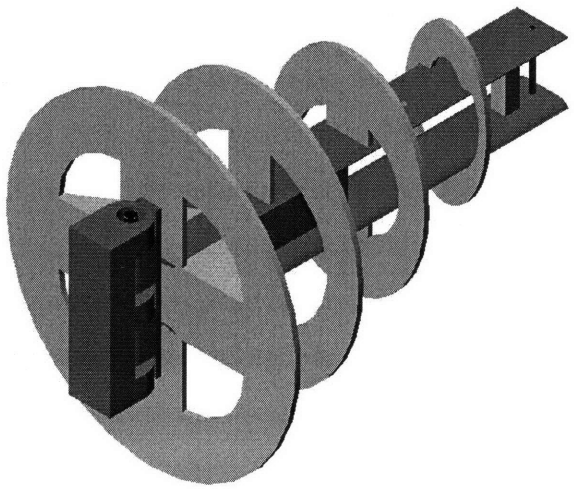

Figure 21: Structural assembly

The moving side of the hinge is bolted to the main tail link bulkhead. Made of aluminum, the circular bulkhead is rigidly attached to the aluminum backbone of the tail. Anchored to the backbone are the ribs, and the hinge for the caudal fin joint. The cross section of the back bone is an I beam shape 3 in. tall by 2.5 in. wide. It can support more than seven times the required load. It was deemed acceptable to remove a section of the beam for the caudal fin actuator because the forces are lower toward the end, and the likelihood that the attachment methods will limit the loading [Appendix D].

6.3 Actuator Choice

In the previous section DC motors and DC linear actuators were identified as the most feasible actuation choices for the set of design requirements set forth. Because they have different specific requirements, the main tail link and the caudal fin link may be driven by either type of actuator. To select a specific actuator, primary attention is paid to the geometrical requirements given above, as well as the MATLAB® analysis which yielded the torque and power requirements of a direct drive actuator. It is assumed that direct drive requirements are the most stringent requirements for the actuator, and that conservative safety factors account for frictional losses that may increase power requirements.

To begin with, a DC motor is the appropriate choice for the main tail link. Quite simply, linear actuators are long, and increase in length as the maximum stroke increases. Some designs are shorter due to an offset axis motor instead of an in line motor, but these designs are bulkier still. The actuator can not be located in the rigid forward section of the vehicle facing aft as it would create unacceptably large dead space, but the problem could be solved by placing the actuator in the moving tail and facing it forward. This approach is good in that it reduces dead space to almost zero, but it has several drawbacks. The anticipated loads and speeds are quite high and continuously repeating. Qualitatively, a screw drive system is better suited to smaller loadings, intermittent use, and precise positioning. Additionally, the large actuator would be off center and interfere with the structural members. Because there is enough allocated space for a rotary motor it makes sense to use it and not make unnecessary sacrifices for unneeded gains.

On the other hand, it makes more sense to actuate the caudal fin link with a linear actuator. Loads on the fin are much smaller, and the required stroke is also smaller. This means a smaller actuator that would have fewer problems fitting among the main link tail structure. A rotary motor would either be located forward in the rigid section and have a long transmission element, or try to convert its rotary motion to linear motion within the confines of a narrowing tail section, which is more easily done in a prepackaged linear actuator.

For the main link rotary motor a search was conducted for a DC brushless motor that operates well at around outputs of 50 Nm of peak torque at powers of 100 to 200 watts, and operates at 48 volts, the present operating voltage of the servo actuators. Motors were considered based on the assumption that they could be pressure compensated for underwater use, appropriate controllers could be contained elsewhere, and that gear heads could be used to slow down motor outputs and generate torque. The result was a massive array of choices and possibilities. The ideal motor characteristics seemed to be just beyond most robotic motion control actuators, and below most heavy industrial motors.

The Tecnadyne Model 60 DC Brushless Rotary Actuator fits the torque, size, and voltage requirements while adding a few bonus features consistent with the commercial-off-the-shelf concept. Offering 136 Nm of torque at 10 rpm, the actuator is compact at 4 in. deep, 4 in. wide, and 8 in. long. It is actually more compact than its dimensions reveal because the shaft is transverse to the length. The unit is designed for underwater applications and is already pressure compensated and contains feedback and control electronics. Furthermore, Tecnadyne specializes in underwater robotics, can supply the actuator in the needed gear ratio [14].

A choice for the caudal fin's linear actuator can also be found in Tecnadyne's product line. The Model 218 DC Brushless Linear Actuator is also pressure compensated for undersea operation which minimizes maintenance concerns. At 12 in. long and 48 volts, it will fit in the tail fin and operate using the standard power source. The Model 218 delivers 250 pounds of force with a 4 in. stroke at 0-2 in. per second, and features a built in pivot mount. This design may be larger than required, but its numerous encapsulated features offset the extra size [14].

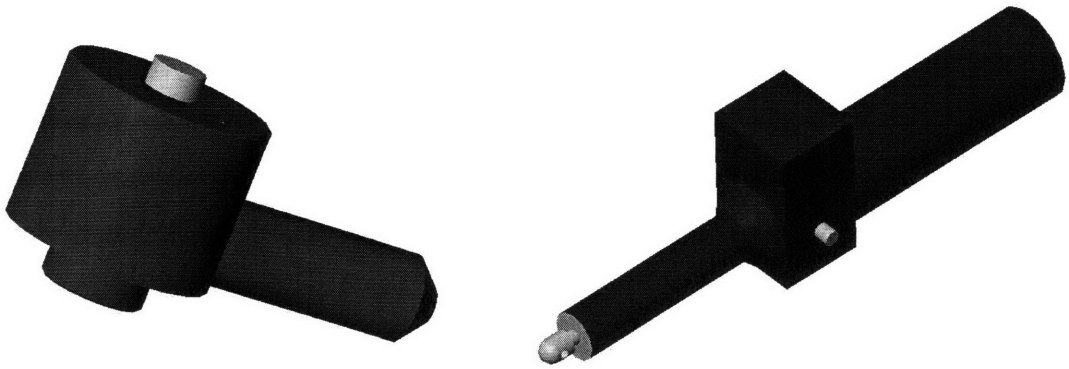

Figure 22: Tecnadyne rotary (left) and linear (right) actuators

6.4 Main Link Mechanism

Previously, pulleys and chains were discussed as power transmission elements for an alternating DC motor. Unfortunately, with such large torques and high frequencies, no motor will last long. Current would constantly be at dangerous levels, causing thermal damage to the motors and possibly harming the vehicle's electrical system. Even so-called "reversing motors" for doors and gates are laden with overload protections and the like, and these devices do not operate at high frequencies. Therefore a mechanism is required to allow the motor to operate at a relatively constant velocity for a given tail beat frequency.

There are several types of linkage mechanism that convert rotary to linear motion. Three of the most common are the crank and slider or rocker, the cam-follower mechanism, and the Scotch yoke. The crank and slider mechanism is used in many applications from engine pistons to windshield wipers. A design incorporating a crank and rocker would have the advantage of not using a sliding surface, but has the drawback of attaching to only one side of the tail structure and taking up a lot of space.

The cam-follower mechanism is a method of reducing the large space requirements of a crank. Figure 23 is a representation of a typical mechanism. The shape of the cam defines the output motion. To use this concept to actuate the main link, the push rod pictured below would be replaced by a lever arm that could apply a torque on

one side of the link. It is conceivable that a second cam attached to the same shaft could actuate the opposite side of the link and make the system symmetrical. The main drawbacks of the cam are the addition of a sliding surface, high fabrication costs, and the addition of a spring to keep the follower in contact with the cam. The versatility of this design is very attractive, because it would allow the swapping of only the cam to change the geometry of output motions if future testing and experimentation should require it. However, the complexity of this design is initially unattractive.

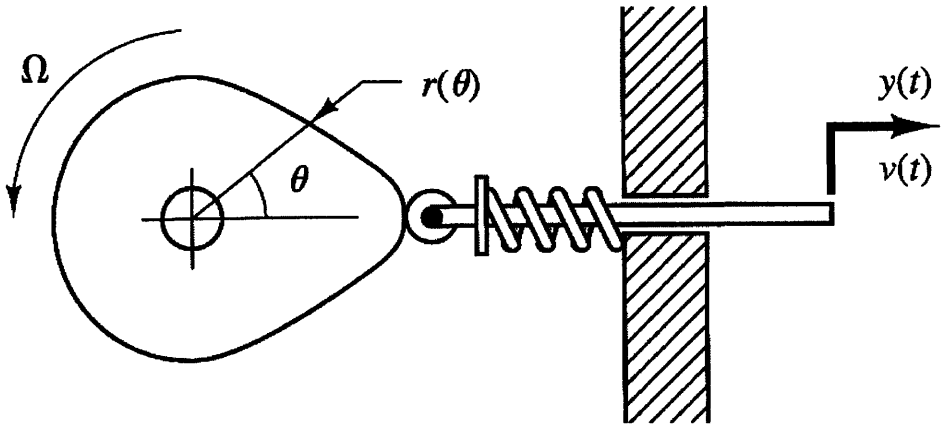

Figure 23: Cam-follower mechanism [21]

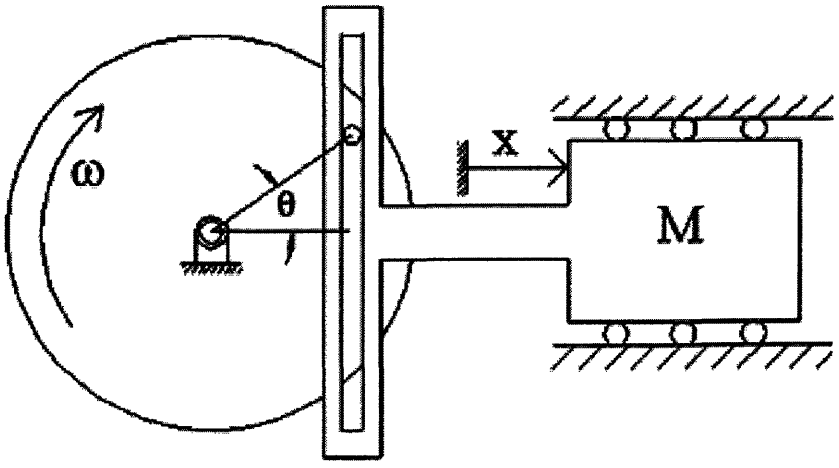

Figure 24: Common Scotch yoke [22]

The Scotch yoke is another common mechanism that combines some of the simplicity of the crank and the compactness of the cam, and is pictured in Figure 24. A disc has a pin attached near its outer radius, which mates with a slider carriage that is constrained to move linearly. As the pin rotates on the disk and translates vertically in the slot, the carriage translates horizontally. The output horizontal linear motion is sinusoidal, which is the desired motion for the main link. The Scotch yoke has a sliding surface that is subject to wear, as does the cam, but is constrained to sinusoidal motion.

The Scotch yoke pictured in Figure 24 looks like it may also require a lever of some sort in order to rotate the main link, but in fact the concept can easily be modified to yield a simple, compact design. Instead of mounting the slot on a linear slide, the slot is rigidly attached to the main link, and causes motion about the hinge. A schematic of the mechanism is shown below. The pin and disk and the hinge are fixed to the front of the vehicle, and the slot and main link rotate about the hinge.

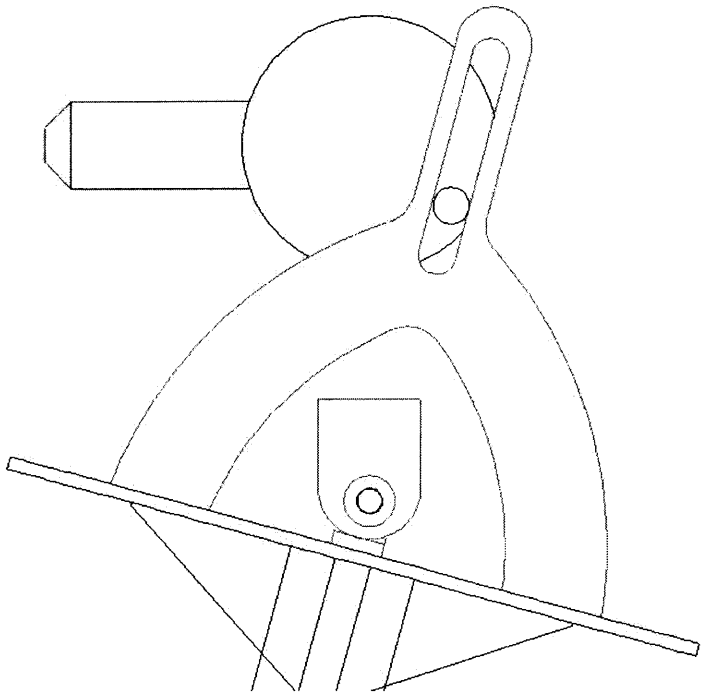

Figure 25: Modified Scotch yoke mechanism

The drawbacks to the modified Scotch yoke mechanism do not outweigh its advantages as a simple design. First, a close inspection of the mechanism's geometry

will show that for a constantly rotating pin, the tail will move in one direction faster than it does the other. This is because the disk rotates 220 degrees between extremes in tail motion going one direction, and 140 degrees in the other. The fluctuation is quantified in Figure 26 below. However, the chosen actuator has an integrated velocity control, which would not require external feedback sensors to provide control. It is worth a complication in the control system to use a simple mechanical system. On the other hand, if a common Scotch yoke was used, a second slider that is also attached to the carriage could provide a pure sinusoidal motion. This approach would defeat the principle on which the modified Scotch yoke was chosen: its simplicity.

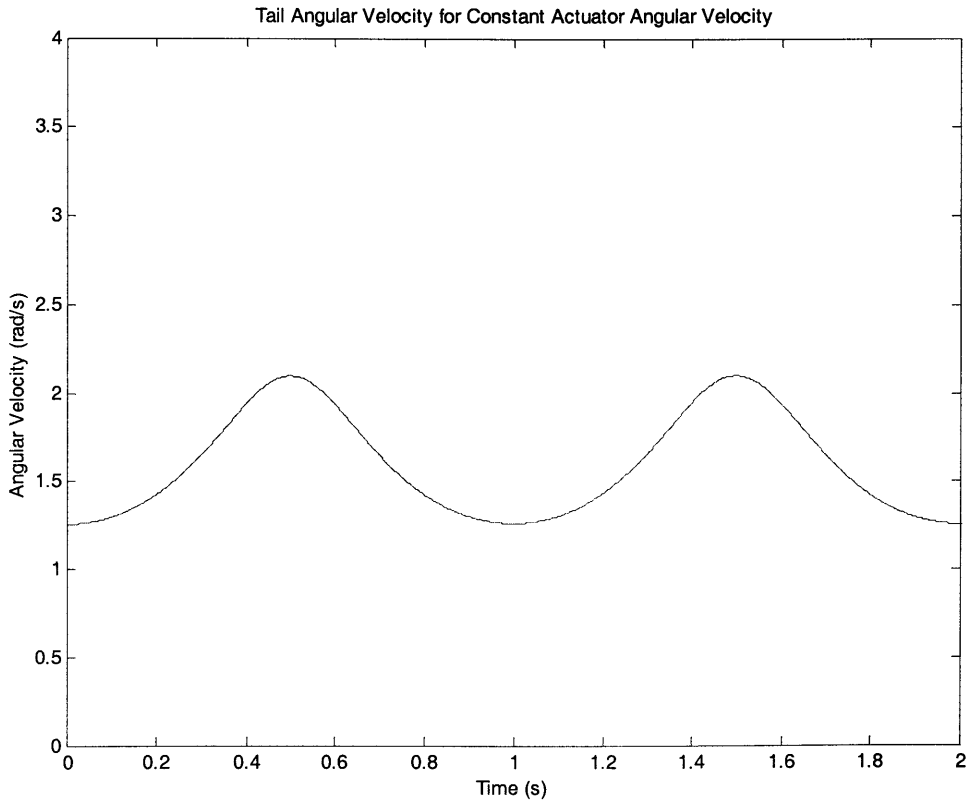

Figure 26: Tail angular velocity for constant actuator angular velocity

The other drawback is the inability to change the motion parameters. In fact, simply altering the pin radius will allow larger tail flapping amplitudes, but it would not allow different motion profiles such as cycloidal motion. However, the central location

of the actuator does not exclude a refit of the system with a cam design in the future. It should be noted that no linkage discussed will allow biasing the flapping motion for turning without the willingness to temporarily oscillate the motor and achieve a smaller amplitude motion. Allowing the tail to remain fully articulated for turning would require using the actuator's encoder for position control.

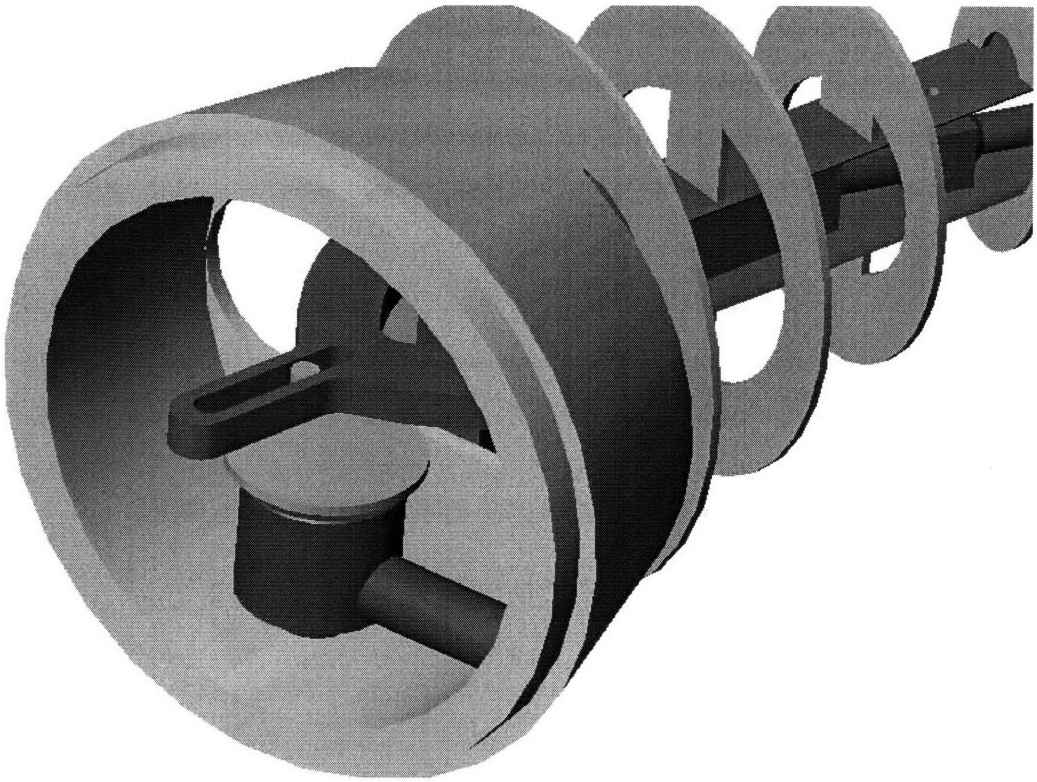

Figure 27: Main link actuator mechanism

The actuator is well suited for the modified Scotch yoke. An analysis of the kinematics of the mechanism was conducted using MATLAB®, and can be found in Appendix E. The analysis was conducted assuming a constant actuator velocity, and therefore reveals the link velocity fluctuations. The model also assumes that the loads on the tail are sinusoidal with a maximum of 50 Nm. This assumption came from the direct drive load analysis discussed earlier, and is an approximation of the total torque curve.

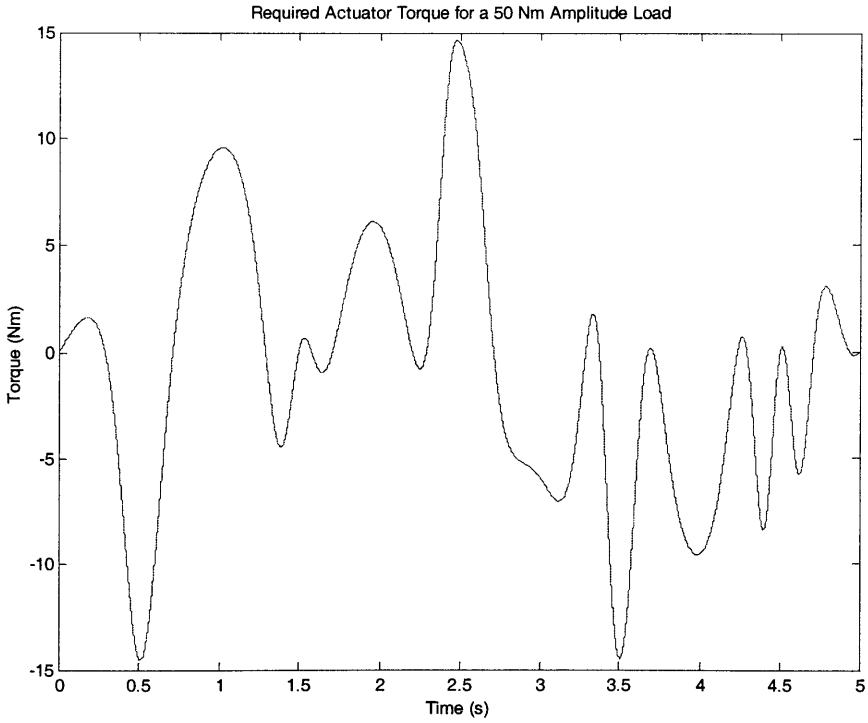

Figure 28: Required actuator torque for a 50 Nm amplitude load

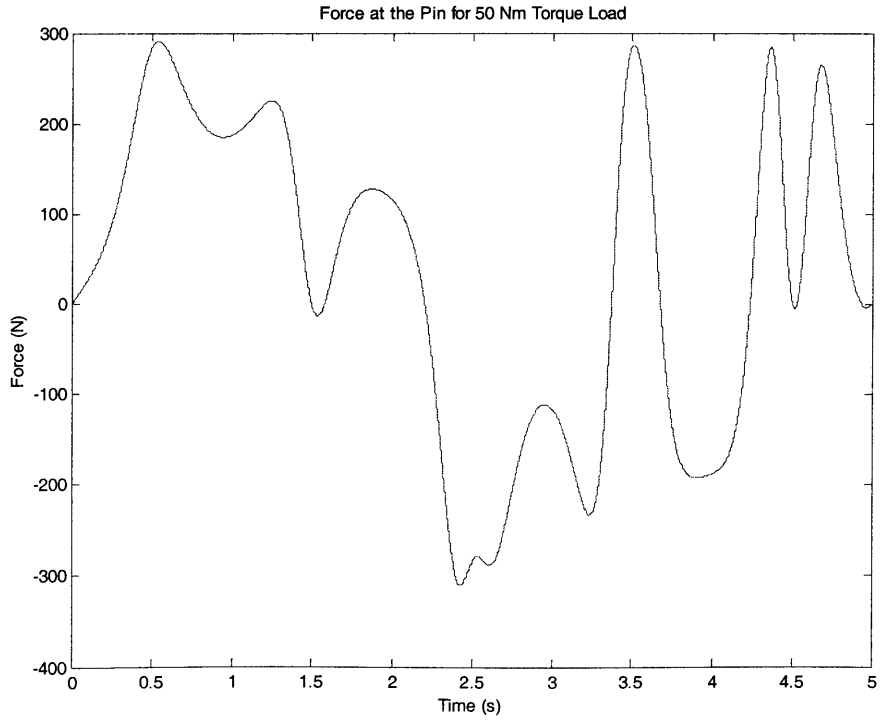

Figure 29: Force at the pin for 50 Nm torque load

At first glance the data in the above figures for required actuator torque and force at the sliding pin seem strange. The result is the effect of a sinusoidal load that is based on an oscillating frequency. The maximum and minimums seen in the plots are indeed the actual values, and they occur consistently over longer time intervals. The peak torque required of the actuator is about 15 Nm. Gearing the actuator to 60 rpm from 10 rpm and 136 Nm gives it about 23 Nm of torque output. A 300 N force at the pin-slider interface is not a concern for breaking the pin.

Material choice for the mechanism is important so that the metals do not corrode, wear, or cause excessive friction. Use of steels will add significant mass to the system and will have to be offset with foam to maintain neutral buoyancy. Aluminum, used in the structure would be a good choice for the slider arm. To combat friction and wear, a replaceable Delrin insert should be machined for the pin-slider interface. These inserts would undoubtedly wear quickly, but could also be replaced very easily. They would also provide a buffer between the aluminum arm and the stainless steel pin to reduce the corrosion that occurs between differing types of metal. Delrin and stainless steel have a low coefficient of friction of about 0.2. The disc could be made of stainless steel as well, and would not corrode the stainless steel shaft of the actuator.

6.5 Caudal Link Mechanism

Caudal fin actuation requires a different approach than the main link. One reason is that space requirements are more stringent due to the narrowing of the tail. This means that there is no large moment arm to push against, but based on the analysis conducted earlier, the caudal fin actuator requires much less force to actuate. The Tecnadyne linear actuator is sufficiently powerful that concerns about reversing the internal motor are minimized.

The mounting scheme is simplified by the actuator's built in pivot point. The I-beam backbone can be cut to make room for the actuator to be mounted along its length. The beam has plenty of stiffness, but if necessary it would not be difficult to reinforce the top and bottom of the beam with additional material to prevent deflection of the mounting holes. The mounting holes can be lined with Delrin bushings for low friction and corrosion protection similar to the pin-slider interface on the main link mechanism.

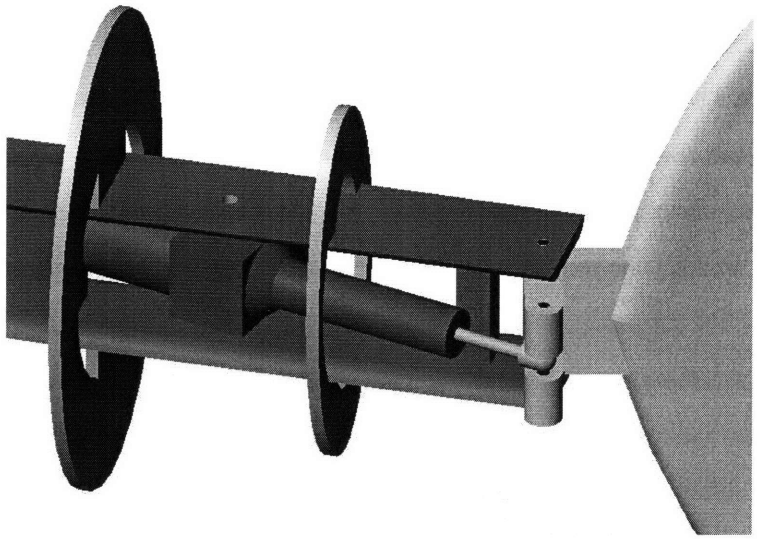

Figure 30: Caudal fin actuation scheme

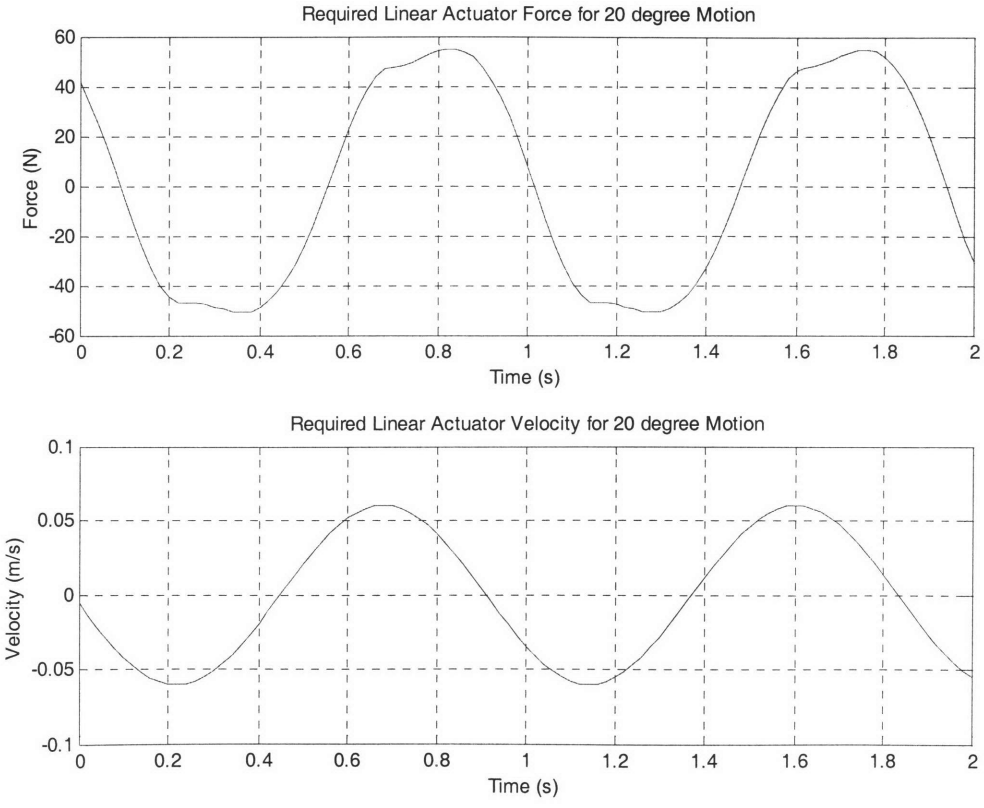

Figure 31: Required force and velocity for the linear actuator

The graphs in Figure 31 present the required force and velocity for the linear actuator configured as shown in Figure 30. The distance from the pivot point to the hinge is 6.9 in. and the moment arm is 1 in. The length from the pivot to the tip of the actuator when the fin is centered is 7 in. The force and velocity model applies the geometry to the direct drive analysis conducted in Section 5, and results in a maximum force of 60 N and a maximum velocity of just over 50 mm/sec. Selecting one of the different gearing options on the Tecnadyne actuator to sacrifice abundant force output for velocity output would put it within operating requirements with room to spare [Appendix C].

6.6 Covering the Tail and Choosing a Caudal Fin

Maintaining smooth flow over the body necessitates an impermeable skin that contains water already inside the flooded sections, and minimizes flow across the interface. The existing fairing material is waterproof but stiff, and making it flexible would require cutting large clearance zones out of it. A flexible skin would allow the motion of the two link tail to be smoothed into a more hydrodynamic shape. The availability of waterproof materials like Gore-Tex® makes a flexible hull feasible.

Figure 32: VCUUV's caudal fin is a NACA 0015 airfoil [20]

The design for flexible skin that holds a smooth shape from the Odyssey main body to the primary tail link uses two separate skins, one tightly stretched over the bulkheads in the tail, and one that is fixed to the Odyssey fairing on one end and loosely stretched over the tail on the other. Two fiberglass battens on each side are stitched into the skin help it to hold its shape. The battens rub against rolling elements in the tail bulkheads (ribs) to reduce friction. The battens extend the percentage of the vehicle that is in motion, but provide additional resistance to the motion of the tail which the actuator must overcome.

The caudal fin has the cross section of a NACA 0015 airfoil. This information was derived from measurements of a real tuna fin during the design of VCUUV, and should be a good approximation of what is necessary for the Odyssey as the vehicles are of similar lengths [15]. VCUUV's fin is shown in Figure 32.

Section 7

Conclusions

7.1 Design Strengths and Weaknesses

A flapping foil retrofit for the Odyssey Class AUV is devised as a way to step up the learning curve toward gaining the full benefits of fish-like propulsion. In the preceding sections, the current methods of propulsion were examined, the prior research that lends the concept feasibility design was studied, design goals were set, various methods of meeting them were explored, and one concept implementation was proposed as a good solution. The proposed solution hopes to achieve a design speed of 1.5 m/s at a tail frequency of about 1 Hz by oscillating two links independently. The links are driven with DC brushless motor systems that drive a Scotch yoke linkage and a linear actuator.

The proposed design's strengths are focused on achieving a robust, practical implementation. The design is simple in several ways. The design's linkages have a low part count, and are large, simple shapes. Also, there are only two actuators (only two power and signal cables), both of which are designed for undersea use and will not limit the environment in which the AUV can operate. The entire mechanical system is self contained, and can be attached directly to the fairing. Furthermore, the heavily loaded actuator is operated in a single direction or rotation, albeit at a fluctuating speed, to increase its lifetime.

Another aspect of the design's practicality is its cost. A retrofit has significant cost savings over a new vehicle design, and the proposed design would be a relatively inexpensive way of testing the flapping foil concept. Cost savings go hand in hand with the idea of minimizing the design's impact on the existing Odyssey design. Although a cost analysis has not been conducted for the parts of the proposed design, it should not be

expensive. The two major foreseen costs are the actuators and the caudal fin itself. Most of the other machining, with the possible exception of the housing, can be done in house.

There are also a few weaknesses with the proposed design. Some of its capabilities have been sacrificed to achieve the strengths discussed above. First, efficiency and motion optimization were disregarded from the outset, and it was assumed that the propulsion system itself would be a subject of study, and that extra power required would still be going to a scientifically useful purpose. Also, the link structure has not attempted to precisely mimic nature, which probably means a loss of efficiency and increased drag. Second, the pressing need to have a motor turn one direction only necessitated a mechanical linkage that limits the ease of changing the swimming parameters. Rather than being changeable in software, there must now be a mechanical swapping of linkage elements. The same one-directional constraint causes difficulty when trying to implement the turning motions. Though these difficulties are not insurmountable, the focus of the vehicle becomes somewhat limited to steady swimming.

7.2 Future Work

Future work on this project should focus on bench-level testing of certain areas of uncertainty while progressing toward building a prototype. The first step would be to produce detailed drawings building on the computer models already made. There are a few choices that remain such as the rotary actuator mount, and whether to weld the structure, or try to make the rib bulkheads adjustable.

The control system should also be addressed. Each actuator incorporates feedback mechanisms in its electronics and contains control circuitry. It should be determined if these systems are adequate, and an interface between them and the main AUV controller (SAIL or newer) must be devised. This controller would ensure that the main link and the caudal link are acting together. Either the actuator electronics or the controller must also maintain the main link actuator at a constant speed. These electronics would probably be located in the control sphere.

Before the actuators are purchased, it would be beneficial to build the main link mechanism and actuate it with other motors on hand to judge its performance under load

and in saltwater. Friction effects, corrosion effects, and material wear properties could be investigated before committing to a gear ratio for the actuators. As the problems are worked out, the rest of the tail can be assembled and tested independently both wet and dry before mounting it in the vehicle.

A field test is the ultimate goal for this project, and the very first task in a serious consideration of the project should be to firmly set the goals of the field test. This thesis has presented a case for one feasible method with general field use in mind, but it should be determined if the choices for the proposed design will accomplish those goals.

References

[1] Blidberg, D. Richard. "The Development of Autonomous Underwater Vehicles; A Brief Summary." Autonomous Undersea Systems Institute, ICRA, Seoul, Korea, May 2001.

[2] Bellingham, James G. "Autonomous Underwater Vehicles." *The Global ABYSS: An Assessment of Deep Submergence Science in the United States,* University-National Oceanographic Laboratory System, Deep Submergence Science Committee.

[3] Bluefin Robotics Website. "AUV Technology." http://www.bluefinrobotics.com/technology.htm

[4] Mandujano, Rafael A. "Odyssey II Tail Cone Design." MIT Sea Grant AUV Laboratory. December 17, 2001.

[5] Dewar, H. and J.B. Graham. "Studies of Tropical Tuna Swimming Performance in a Large Water Tunnel, Part III: Kinematics." *Journal of Experimental Biology*, Vol. 192, 1994, pp. 45-59.

[6] Barrett, D.S., *Propulsive Efficiency of a Flexible Hull Underwater Vehicle*. PhD Thesis, Ocean Engineering, Massachusetts Institute of Technology, 1996.

[7] Anderson, J.M., K Streitlien, D.S. Barrett, and M.S. Triantafyllou. "Oscillating Foils of High Propulsive Efficiency." *Journal of Fluid Mechanics*, Vol. 360, 1998, pp. 41-72.

[8] Anderson, J.M., P.A. Kerrebrock, and M.S. Triantafyllou. "Concept Design of a Flexible-Hull Unmanned Undersea Vehicle." *Proceedings of the 7th International Offshore and Polar Engineering Conference*, Vol.II, Honolulu, Hawaii, May 25-30, 1997, pp. 82-88.

[9] Anderson, J.M., P.A. Kerrebrock. "The Vorticity Control Unmanned Undersea Vehicle [VCUUV]: An Autonomous Robot Tuna." *11th International Symposium on Unmanned Untethered Submersible Technology,* Durham, NH, August 23-25, 1999.

[10] Fox, R.W., and MacDonald, A.T. *Introduction to Fluid Mechanics, Fifth Edition.* New York:Wiley, pp. 442-473.

[11] Barrett, D.S., *The Design of a Flexible Hull Undersea Vehicle Propelled by an Oscillating Foil.* M.S. Thesis, Ocean Engineering, Massachusetts Institute of Technology, 1994.

[12] Tolkoff, S.W., *Robotics and Power Measurements of the RoboTuna.* M.S. Thesis, Ocean Engineering, Massachusetts Institute of Technology, 1996.

[13] Daviss, Bennett. *New Scientist.* "Jet-Propelled Tuna." March 4, 2000. http://www.bluefish.org/jettuna.htm

[14] Tecnadye website. http://www.tecnadyne.com

[15] Anderson, J.M., P.A. Kerrebrock. "The Vorticity Control Unmanned Undersea Vehicle (VCUUV): An Autonomous Vehicle Employing Fish Swimming Propulsion and Maneuvering." *10th International Symposium on Unmanned Untethered Submersible Technology,* Lee, NH, September 7-10, 1997.

Photo Credits

[16] MIT Sea Grant Autonomous Underwater Vehicle Laboratory website. http://auvlab.mit.edu

[17] Bauman's Moscow State Technical University website. http://aqua.sm.bmstu.ru

[18] Bluefin Robotics website. http://www.bluefinrobotics.com

[19] MIT Tow Tank website. http://web.mit.edu/towtank/www/tuna/brad/design3.html

[20] Draper Laboratory website. http://www.draper.com/tuna_web/vcuuv.htm

[21] Dynamic Systems Modeling and Controls Laboratory, University of Washington website. http://abs-5.me.washington.edu/dynlab/

[22] Tribology Laboratory, University of Florida website. http://grove.ufl.edu/~wgsawyer/Laboratory/Wear/Mechanisms.HTML

Appendix A

Sizing Body and Tail Length

```
% Scheme for determining overall length
% mod 5-06-02 Rafael Mandujano

clear all;
figure(1);
clf;
hold on;

% Examine the body length between 82 and 100 inchees
BL = linspace(82,100);
% Dead Length - post to hinge length
DL = 73; % 73" (10" of dead space)
% Tail length
TL = BL - DL;
% Required peak-to-peak fin amplitude at three factors
A_req = 0.11*BL;     % Robotuna optimum
A_req2 = 0.15*BL;    % Lower biological range
A_req3 = 0.2*BL;     % Upper biological range
% Plot of several angle amplitudes starting at 15 degrees in 5 deg
increments
for i = 1:5,
    theta = (10 + 5*i) * (pi/180);
    A = 2 * (TL * sin(theta));
    plot(BL,A,':');
end

% Plot
plot(BL,A_req,'g',BL,A_req2,'r',BL,A_req3,'b',BL,TL,'-');

plot(93, 20,'*');
ylabel('Peak to Peak Caudal Amplitude or Length (in)');
xlabel('Body Length (in)');
title('Sizing the Tail and Angle Amplitude - Choose 20deg Amplitude,
for a 93" BL and 20" TL');
hold off;

% Selection Criteria
% Choose the smallest amp to minimize drag due to forward motion, but
% within a reasonable length
```

Appendix B

System Model for Main Link

```
% Main link model
% mod 4-26-02 Rafael Mandujano

clear all;

% Design for these three parameters
BL = 93 * .0254
TL = 20 * .0254                 % Tail length (hinge-precaudal)
U = (0.65 * BL)                 % m/s vehicle velocity
St = 0.25;
A = 0.15 * BL;                  % Amplitude of caudal fin

% The above parameters dictate that we should oscillate the tail at
TBF = (St * U) / A              % Hz  tail beat frequency
% Note that increasing frequency scales linearly with the velocity

% Now lets model the tail characteristics as best we can
% Lets assume neutral buoyancy in a waterproof skin
% Lets also say that the tail is made of 4 elliptical-cylindrical
sections

% Lumped parameter model for each section
d = 0.0254 * [3.5 8.5 13.5 18.5]; %distance from hinge to center mass
delta = 0.0254 * 5;

a = [7.5 6.25 5 3.75] * 0.0254    % major axis - vertical
b = [7 5.25 3.75 2] * 0.0254      % minor axis - horz

A_section = pi * (a .* b);
V = (delta) * A_section;

rho = 1000;
m = rho*V;                      % mass assuming neutral buoyancy
m_added = 0.3*m;                % added mass safety factor
m_dyn = m + m_added;
m_fin = 0.75 * (0.65 * .13 * .02) * 1800; % estimated mass of a
                                % fiberglass caudal fin based on VCUUV's
I = m_dyn .* d.^2
I_fin = m_fin * (TL)^2;
Io = sum(I) + I_fin;  %Result is a linear sum of the moments of inertia

% Main link dynamics
w = 2 * pi * TBF;
t = [0:0.02:2];

theta = A * sin(w*t);
thetadot = A * w * cos(w*t);
theta2dot = - A * w^2 * sin(w*t);
```

```
tau = Io .* theta2dot;          % Inertia torque

Cd = 0.4;                       % For a cylinder of Re ~= 5*10^5
for i = 1:4
    torque(i,:) = Cd * 0.5 * (a(i) * delta) * 1000 .* d(i).^2 *
thetadot.^2 .* d(i) .* sign(thetadot);  %%%%%
end
tau_drag = sum(torque);         % Drag torque


% Rough estimate of the lifting, drag forces from the oscillating fin
that
% are transmitted to the main link
Cd_fin = 1;                     % Flat plate
fin_drag = Cd_fin * 0.5 * (0.75*(0.13 * 0.65)) * 1000 * (TL)^2 *
thetadot.^2 * (TL) .* sign(thetadot);
torque(5,:) = fin_drag;

tau_drag = sum(torque);

% Power calculations
dragpow = tau_drag .* thetadot .* sign(thetadot);
inerpow = tau .* thetadot;
power = dragpow + inerpow;

% Inertial load will require maximum torque at the amplitude maxes
% Drag will always oppose the motion and will cause no torque at the
maxes, but will increase
%   torque requirements while the link is in motion

figure(1);
clf;
subplot(211);
plot(t,tau,'--',t,tau_drag,'-.',t,tau+tau_drag,'-',t,theta*50,':');
legend('Inertial torque','Drag torque','Total torque', 'Fin Position
(x50)');
title('Direct Drive Torque Requirements for Flapping Tail');
ylabel('Torque (Nm)');
xlabel('Time (s)');
grid on;

subplot(212);
plot(t,power,'-',t,dragpow,'-.',t,inerpow,'--',t,theta*50,':');
title('Direct Drive Power Requirements for Flapping Tail');
ylabel('Power (W)');
xlabel('Time (s)');legend('Total power','Drag power','Inertial
power','Fin Position (x50)');
grid on;
```

Appendix C

System Model for Caudal Link

```
% Caudal fin model
% mod 4-29-02 Rafael Mandujano
clear all;

BL = 93*.0254
U = (0.65 * BL) % m/s vehicle velocity
St = 0.25;
A = 0.15 * BL; % Amplitude of caudal fin
TBF = (St * U) / A % Hz  tail beat freqency

w = 2 * pi * TBF;
t = [0:0.02:2];

theta2 = A * sin(w*t);
thetadot2 = A * w * cos(w*t);
theta2dot2 = - A * w^2 * sin(w*t);

% Estimated mass of a fiberglass caudal fin based on VCUUV's
m_fin = 0.75 * (0.65 * .13 * .02) * 1800;
center = 0.18;
I_fin = m_fin * center^2;
tau = I_fin * theta2dot2;
% Estimated drag on fin as a flat plate
Cd = 1.0; % From a flat plate
tau_drag = Cd * 0.5 * (0.75*(0.13 * 0.65)) * 1000 * (center)^2 *
thetadot2.^2 * (center) .* sign(thetadot2);

% Linear actuator method
% Force, speed for actuator

% Define max angle of attack
max_theta = 20 * (pi/180);

phi = 95 * (pi/180); % from Robotuna
theta_fin = max_theta * sin(w*t+phi);
theta_findot = w * max_theta * cos(w*t+phi);

% Arm radius space limited so define as
d_arm = 1 * 0.0254;

% Define limits of actuator extension
extend_min = 5.953 * 0.0254;
extend_max = 9.953 * 0.0254;
extend_neu = 7 * 0.0254;

% Find distance from caudal hinge to actuator pivot
% based on neutral position
d_pivot = sqrt((extend_neu)^2 - (d_arm^2))
```

```
extension = sqrt(d_arm^2 + d_pivot^2 - (2*d_arm*d_pivot*cos((pi/2)-
theta_fin)));
alpha = asin((d_arm*cos(theta_fin))./extension);

% Forces and torques

F_perp = ((tau+tau_drag) / d_arm);
F_req = F_perp .* cos(alpha - theta_fin);

% Velocities

v = d_arm * theta_findot;

% Power

iner_pow = tau .* w;
drag_pow = tau_drag .* w;
tot_pow = iner_pow + drag_pow;

figure(3);
clf;
subplot(212);
plot(t,iner_pow,'--',t,drag_pow,':',t,tot_pow,'-');
title('Direct Drive Power Requirements for Caudal Fin');
xlabel('Time (s)');
ylabel('Power (W)');
legend('Inertial Power','Drag Power','Total Power');
grid;
subplot(211);
plot(t,tau,'--',t,tau_drag,':',t,tau+tau_drag,'-');
title('Direct Drive Torque Requirements for Caudal Fin')
xlabel('Time (s)');
ylabel('Torque (Nm)');
legend('Inertial Torque','Drag Torque','Total Torque');
grid;

figure(4);
clf;
subplot(211);
plot(t,F_req);
title('Required Linear Actuator Force for 20 degree Motion');
xlabel('Time (s)');
ylabel('Force (N)');
grid;
subplot(212);
plot(t,v);
title('Required Linear Actuator Velocity for 20 degree Motion');
xlabel('Time (s)');
ylabel('Velocity (m/s)');
grid;
```

Appendix D

Structural Calculations

```
% Structural and miscellaneous mechanical loading calculations
% mod 4-22-02 Rafael Mandujano

% Determine the necessary I beam size

% Vertical load beam bending lumped point loads along beam and at tip
% Based on full water weight in air
E = 69e9;                    % GPa Aluminum
stress_max = 0.75 * 255e6;   % Yield of Aluminum with Safety factor 1.33
defl_max = 0.001;            % Half the no deflection condition
g = 9.8;

rho = 1000;
a = 6 * 0.0254;
b = 6 * 0.0254;
A_section = pi * (a .* b);
TL = 20 * 0.0254;

w = (A_section * rho) * g;  % Load per length
P = 0.75 * (0.65 * .13 * .02) * 1800 * g; % Point load of caudal fin

% Cantilever beam bending equations
% Vertical
I_req_w = (3*w*TL^4) / (24*E*defl_max);
I_req_P = (P*2*TL^3) / (6*E*defl_max);
I_req = I_req_w + I_req_P

% Horizontal
I_req_horz = (70*2*TL^3) / (6*E*defl_max) % Load value taken from
plant.m script

% A 3" height, 2.5" width standard aluminum I beam has a
% moment of inertia of 9.32e-7 m^4 at 0.74 kg per foot for vertical
bending
% and 2.16e-7 for horizontal bending

% No yield condition
% Vertical torque if vehicle is pulled out of water filled
g = 9.8;
tau_vert = (w * TL^2 / 2) + (P*TL);
beam_height = 3 * 0.0254;
I_noyield = tau_vert * (beam_height/2) / stress_max

% Radial loads on a 2 point hinge joint
hinge_height = 6 * 0.0254;
load_hinge = (2*tau_vert/hinge_height)
```

Output of the script:

```
>> findi

I_req =

  1.3997e-007


I_req_horz =

  4.4332e-008


I_noyield =

  2.9068e-008


load_hinge =

  1.9149e+003
```

Appendix E

Modified Scotch Yoke Model

```
% Model for modified Scotch yoke for use with the main link
% mod 4-26-02 by Rafael Mandujano

d = 2 * 0.0254;
L = 8 * 0.0254;

theta_max = 20 * (pi/180);      % maximum angle of tail fin
tau_max = 50;                   % max torque from direct drive model
(assume sinusoidal)

t = linspace(0,5,10000);
w_m = 2 * pi;                   % constant velocity motor
theta_m = w_m * t;

x_pin = d * sin(theta_m);       % coordinates at center of motor
rotation
y_pin = d * cos(theta_m);

r = sqrt( x_pin.^2 + (L + y_pin).^2);

v_pin = d * w_m;
w = v_pin ./ r;                 % equate linear vel at sliding point

% Load model at hinge frame of reference
tau_load = tau_max .* sin(w.*t);
F_load = tau_load ./ r;

theta = atan((d*sin(theta_m))./(L+d*cos(theta_m)));
d_eff = d * cos(theta_m - theta);   % effective radius of the pin
acting on the slot

tau_req = F_load .* d_eff;

plot(t,w);
title('Tail Angular Velocity for Constant Actuator Angular Velocity');
ylabel('Angular Velocity (rad/s)');
xlabel('Time (s)');
axis([0 2 0 4]);
```